Coordination Chemistry Reviews 436 (2021) 213791

Contents lists available at ScienceDirect

Coordination Chemistry Reviews

journal homepage: www.elsevier.com/locate/ccr

Review

From binary to multinary copper based nitrides – Unlocking the potential of new applications

Aleksandra Ścigała [a], Edward Szłyk [a], Liliana Dobrzańska [a], Duncan H. Gregory [b], Robert Szczęsny [a,*]

[a] Faculty of Chemistry, Nicolaus Copernicus University in Toruń, Gagarina 7, 87-100 Toruń, Poland
[b] WestCHEM, School of Chemistry, University of Glasgow, Glasgow G12 8QQ, United Kingdom

ARTICLE INFO

Article history:
Received 15 October 2020
Received in revised form 9 January 2021
Accepted 10 January 2021
Available online xxxx

Keywords:
Copper nitride
Chemical methods
Synthesis
Applications
Ternary copper nitrides
Quaternary copper nitrides
Thin films

ABSTRACT

This review summarizes the current knowledge on the chemistry of binary copper(I) nitride, Cu_3N and its multinary derivatives containing either main group or transition metal elements. For many years, research in this area was focused on the development of copper nitride prepared in the form of thin films. Successful deposition of these materials has been achieved mainly by employing physical methods, which have provided materials suitable for potential application in optical data storage. However, for the last decade, attention has also been devoted to expanding the available options by which Cu_3N can be synthesized and deposited. Consequently, the focus has switched to the development of chemical synthetic methods towards the fabrication of this semiconductor and to broadening the range of related compounds that might be discovered. Simultaneously, the formulation of novel techniques and the successful preparation of new nanostructured functional materials has resulted in the rapid evolution of new and relevant applications; e.g. catalytic and electrochemical. The overview presented here concentrates on the chemical methods that have been devised to synthesise both bulk samples and thin films of Cu_3N. Our article also shows how these approaches have been developed to achieve significant progress in the creation of multinary copper based nitrides and in identifying their potential applications. It provides a concise history of previous copper nitride research and sets the context for the most current advances. These will no doubt provide the springboard for future research areas that will impact both transition metal nitride chemistry and materials science more generally.

Contents

1. Introduction . . . 2
2. Binary copper nitride . . . 3
 2.1. Synthesis strategies to copper nitride powders . . . 3
  2.1.1. Ammonolysis reactions . . . 3
  2.1.2. Solution-based synthesis . . . 6
  2.1.3. Solid state synthesis . . . 10
 2.2. Thin films of copper nitride . . . 10
  2.2.1. Physical deposition methods . . . 10
  2.2.2. Chemical deposition methods . . . 11
 2.3. Properties and applications of binary copper nitride . . . 12
3. Multinary copper-based nitrides . . . 14
 3.1. Preparation and structural characterisation . . . 15
  3.1.1. Ternary copper nitrides . . . 15
  3.1.2. Quaternary copper nitrides . . . 17
 3.2. Properties and applications . . . 17
4. Conclusions . . . 18

* Corresponding author.
E-mail address: roszcz@umk.pl (R. Szczęsny).

https://doi.org/10.1016/j.ccr.2021.213791
0010-8545/

Declaration of Competing Interest 19
Acknowledgement 19
References 19

1. Introduction

In recent years, there has been growing interest in the chemistry of nitrides [1–4]. The progress in this field not only concerns developing new or modified methods of synthesis and deriving the structures of these compounds, but also exploring previously unknown, useful applications for both bulk and nanostructured nitrides. Many binary nitrides from the periodic table have been characterized in depth. Increasingly, detailed analysis has also been extended to multinary systems, which have already been shown to exhibit tremendous compositional and structural diversity [5–10]. Scientific reports are still continuously expanding the scope of applications for this broad class of binary and higher compounds. Nitrides such as TiN [11,12], Si_3N_4 [13,14], and BN [15,16] are utilized as materials with high resistance to heat, or materials with remarkable hardness. Gallium nitride is widely used in optoelectronic technologies [17,18] and lithium nitride is capable of reversible hydrogen sorption and, when doped, can be employed for hydrogen storage [19,20] or as an anode material in Li-ion batteries [1,21,22]. Nitride-based materials also warrant study from the perspective of basic science, because they constitute a relatively unexplored and very diverse class of inorganic compounds, compared to oxides which have been studied more extensively in the past decades. In the family of transition-metal nitrides, studies have focused mainly on the thermodynamically stable binary nitrides formed by the early transition metals from groups 3 to 6. In recent years, less thermally stable transition-metal nitrides (often containing the later transition metals from groups 7 to 12), which are more difficult or even impossible to obtain by conventional high-temperature synthetic methods, have become the subject of more extensive research [23]. Copper nitride, Cu_3N, is one such example.

This review attempts to offer a comprehensive compilation of research related to the chemistry of copper nitrides, covering synthetic methods, as well as structural and physicochemical properties of these promising functional materials. Copper nitride itself appears at first sight to be a rather simple cubic compound with an *anti*-ReO_3 type structure (space group $Pm\bar{3}m$) in which nitrogen ions occupy the corners of the primitive unit cell and copper ions are located at the center of the cubic edges (Fig. 1) [24]. This type of open, low density crystal structure would seem to be a perfect candidate for intercalation and in fact the structure is well-suited for the insertion of metal atoms at the interstitial body center site (½,½,½) under certain conditions [25,26]. The insertion of additional metallic elements results in alteration of the chemical interactions between the copper and nitrogen atoms, which significantly affects the electronic structure of the material. In particular, experimental and computational studies revealed that Cu_3N character changes to metallic as a result of doping [25,27,28]. It is worth mentioning that although copper(I) nitride itself has been studied quite extensively over a long period of time, there are still some significant gaps in the knowledge of the parent material, for example, even the size of the electronic band gap for Cu_3N is still not firmly established and is reported, presumably also by inconsistent terminology, across a surprisingly wide range of values from 0.23 to 1.90 eV. These apparent disparities are reasons alone for further systematic research in the future [29]. It also shows that the chemistry and physics of copper nitride are still far from rationalised and that copper nitride presents challenges for both disciplines that in turn could impact materials science and engineering. Recently, computational methods have been central in correlating the thermodynamic properties of copper nitride with its structure and bonding, as well as in predicting new related materials that are yet to be discovered experimentally [27,30].

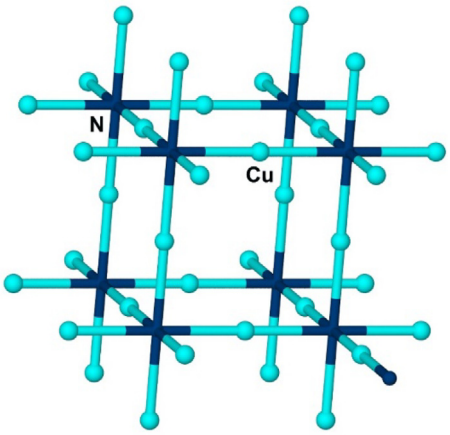

Fig. 1. The cubic, *anti*-ReO_3 type crystal structure of copper nitride, Cu_3N. N (dark blue) occupies the corner sites of the primitive unit cell with Cu (light blue) occupying the edge positions.

For such a seemingly simple compound, research on copper nitride has proven to be multi-faceted and despite the lingering uncertainties surrounding its chemical and physical properties research has already branched off to consider the possibility of creating thin films of Cu_3N. Investigations of nanostructured 2D Cu_3N layers starting from preparation, fabrication and characterization [29], soon progressed to consider applications, for example in the technology of write-once optical data storage [31,32], magnetic tunnel junctions [33] or opto-electronic devices, e.g. photodetectors [34]. Cu_3N film deposition can be used also as a route to printing 1D microscopic copper lines and dots with intended uses in miniaturised electronic devices [35]. This latter usage is facilitated by the fact that copper nitride can be easily thermally decomposed into nitrogen and pure metal (decomposition temperature: 350 °C), as characterized by the material's significantly higher reflectivity and conductivity [36,37]. The above-mentioned films were each fabricated by one of a variety of physical methods, the most commonly used being RF magnetron sputtering [37–42]. Pulsed laser deposition [43,44], molecular beam epitaxy [33,45], atomic layer deposition [46], ion-assisted deposition [47] or DC triode sputtering [48,49] are also among the physical deposition techniques that have been successfully applied. In fact, the Cu_3N films that have been reported to have been fabricated by these methods are not always consistent in their nominal stoichiometry. Often referred to in the literature more broadly as a family of Cu–N compounds, the electronic properties of these materials varies considerably with chemical composition, ranging from copper-rich Cu_4N which is metallic to Cu_3N, which demonstrates the expected semiconducting behavior. Films thus apparently exist as stoichiometric (Cu_3N) or either in nitrogen-rich or copper-rich forms [29,50,51]. Reports suggest that the film stoichiometry can be tuned by

changing the deposition conditions [52]. Furthermore, the physical properties of deposited Cu_3N thin layers could be manipulated by including additional elements within the films, such as alkali metals (lithium), transition metals (Ti, Pb, Ni, Zn, Cr, Fe, Mn, Al and Sc) or non-metals (H and O) [53].

Despite the fact that chemical synthesis routes to obtain powders of Cu_3N predate the above-mentioned thin films studies by several decades [54], they were represented by relatively little research until the end of the first decade of the 21st century. A sizable increase in the number of new synthesis methods, mainly devoted to the production of copper nitride nanoparticles, were reported at this time. The effect of this was to unlock new and potentially useful applications for copper nitride that could take advantage of both its physical and chemical properties. New research areas are emerging in which the catalytic and electrochemical properties of copper nitride have come under scrutiny. For example, Cu_3N has been proposed as an inexpensive alternative to Pt/C catalysts for the oxygen reduction reaction (ORR) [55], as an effective new conductive ink [56] and as material useful for rechargeable Li-ion batteries [57,58]. Moreover, there are the additional possibilities of using Cu_3N as a starting material to new and more complex nitrides. The often otherwise-challenging syntheses of multinary nitrides considerably broadens the potential of binary nitrides such as Cu_3N as such starting materials (e.g. the use of Cu_3N to prepare nanocrystals of the *anti*-perovskite, Cu_3PdN is just one example) [59].

In light of the many developments in the chemistry of Cu_3N and of higher copper nitrides, it is timely to collate these advances and to place them into a wider historical context. In fact, to the best of our knowledge, this article represents the first comprehensive review to present a systematic and critical assessment of the chemistry and materials science of copper nitrides. It brings together essential information on structure, properties and, importantly, the growing corpus of chemical synthetic pathways to copper nitrides. Selected examples from experimental and some theoretical studies are discussed to demonstrate the function of these materials and to show how they find application.

Following this introduction, the review begins by considering the various techniques by which first bulk powders and secondly, thin films of copper nitride, might be fabricated. The growing number of choices that one can make in adopting a preferred synthesis method has important implications for the structure of Cu_3N across length scales and this is reflected in the following section which considers these effects on properties and the lead-in to applications. The article then turns to systems of higher compositional complexity and the chemistry of the ever-growing tranche of ternary and higher copper nitrides. The synthesis, crystal structures and known properties of these nitrides are presented in detail with reference to theoretical studies and to cases where higher nitrides have been characterised and tested experimentally. We finish by considering the many possible future directions for copper nitride research and development before drawing the article to a conclusion.

2. Binary copper nitride

2.1. Synthesis strategies to copper nitride powders

Gaseous dinitrogen is widely perceived to be inert, with a triple bond that is exceptionally difficult to break, especially when compared to dioxygen, for example (the BE for N_2 is 945 kJ mol^{-1}, whereas for O_2 it is 498 kJ mol^{-1} [60]). Metastable nitrides therefore need to be prepared from nitrogen-containing precursors which exhibit higher activity/reactivity than the N_2 molecule itself. Chemical ways to introduce nitrogen as nitride without recourse to extreme conditions, rely on using less thermodynamically stable nitrogen compounds, such as ammonia (NH_3) in the gaseous or liquid phase or azides in the solid state [61].

The general synthesis method of copper nitride is thus based on the reaction of a copper precursor with a nitriding agent, often above ambient temperature. Among the reported preparation methods of Cu_3N, the most comprehensive are either solid–gas reactions, where a solid copper-containing precursor reacts with a gaseous high activity nitrogen source or solution-based techniques, which are performed in non-aqueous solvents.

2.1.1. Ammonolysis reactions

The most commonly-used method for the synthesis of binary late transition metal nitrides is the ammonolysis reaction of a metal precursor with gaseous ammonia. Such reactions are performed at moderate temperatures in solid state chemistry terms (typically < 500 °C) and require air (oxygen and water) to be excluded at all times during synthesis and handling. Ammonolysis reactions are usually optimised by varying the temperature, reaction time, heating/cooling rate, ammonia flow rate and/or choice of solid state precursor. Cu_3N, in similarity to many other late transition metal nitrides, thermally decomposes at relatively low temperature and so the reaction temperatures in such ammonolysis processes are severely limited. The first reported synthesis of copper(I) nitride was achieved by ammonolysis and was performed by Juza and Hahn in 1938. In this case, a solid precursor of copper(II) fluoride (CuF_2) was heated under a flow of gaseous ammonia to 280 °C for 3 h (Table 1). On the basis of X-ray diffraction measurements, the authors determined the crystal structure of Cu_3N powder as *anti*-ReO_3 [54,62]. Gregory *et al.* utilized the same precursor and obtained a single-phase Cu_3N powder consisting of submicron plate-shaped particles (Fig. 2a). The phase-pure material was achieved within a temperature range of 250–325 °C over periods of 6–45 h (NH_3 flow rate: 500–700 ml/min). Above 325 °C, however, although the major product remained as Cu_3N, the powder began to show traces of Cu metal impurity, whereas at 400 °C copper nitride had completely decomposed to metallic copper [24]. In this work, the authors used a combination of powder X-ray diffraction (PXD) and powder neutron diffraction (PND) techniques to obtain a definitive structural model for Cu_3N and to confirm the fully stoichiometric composition of the binary phase. The ammonolysis process was recommended as a convenient route for the reproducible synthesis of large amounts of high-purity Cu_3N.

Many recent studies have demonstrated how Cu_3N powders can be similarly synthesized using various other copper-containing precursors. In many cases, by selecting an appropriate precursor and suitable reaction conditions it is possible to produce Cu_3N nanoparticles, either in supported or unsupported forms. Lee *et al.* synthesized Cu_3N nanoparticles of ~ 22 nm diameter, which were supported on mesoporous materials (Fig. 2b) in a two-step synthesis involving impregnation followed by ammonolysis. A precursor of $Cu(OAc)_2{\cdot}H_2O$ was impregnated into $Fe_3N@SiO_2$ microspheres that had been previously prepared by similar impregnation methods using iron precursors supported on silica spheres. The acetate-coated $Fe_3N@SiO_2$ microspheres were then heated at 250 °C for 6 h in a mixed NH_3/N_2 atmosphere (NH_3: N_2 = 7:3) to yield the corresponding supported copper nitride nanoparticles [63]. The activity of the final $Cu_3N/Fe_3N@SiO_2$ catalyst was tested towards the Huisgen 1,3-dipolar cycloaddition (HDC) of azides and alkynes. Li *et al.* compared two different precursors to prepare the nitride powder; copper(II) fluoride and copper(II) pivalate ($Cu(OPiv)_2$). Ammonolysis of CuF_2 (dried at 140 °C for 6 h under flowing nitrogen) was performed at 300 °C for 8 h and resulted in the formation of large, dense particles with a refined crystallite size of 412 ± 11 nm. In contrast, the ammonoly-

Table 1
Methods and conditions for the various synthesis routes to Cu_3N powders complete with a description of the morphology and size of the resulting crystallites.

Method	Precursors/Substrates	Conditions	Shape/Morphology	Size / nm		Ref.
				XRD	TEM/SEM	
Ammonolysis	CuF_2, NH_3 gas	280 °C, 3 h				[54,62]
	CuF_2, NH_3 gas	250–325 °C, 6–45 h, NH_3 flow rate: 500–700 ml/min	plate- and ill-shaped particles		< 1000	[24]
	$Cu(OAc)_2{\cdot}H_2O$ (incorporated to $Fe_3N@SiO_2$), NH_3/N_2 gas	250 °C, 6 h, (NH_3:N_2 = 7:3)	spherical particles supported on SiO_2 shell	22.4		[63]
	CuF_2, NH_3 gas	300 °C, 8 h	dense particles	412 ± 11		[67]
	$Cu(OPiv)_2$, NH_3 gas	180–300 °C, 10 h	aggregated particles	51.3 ± 1	20	[67]
	$Cu(CF_3COO)_2$, NH_3 gas	250–350 °C, 45 min-5 h	dense, ill-shaped particles		< 500 (particles)	[64]
	$CuSiO_3$, NH_3 gas	350 °C, 1 h, NH_3 flow rate: 10 l h^{-1}	spherical particles on SiO_2 surface	31	~ 100	[65]
	CuO@SiO_2 (obtained from $Cu(NO_3)_2$/CS/SiO_2), NH_3 gas	300 °C, 10 h, NH_3 flow rate: 10 l h^{-1}	irregular particles encapsulated in SiO_2 spheres	17	<30	[65]
	CuO@SiO_2 (obtained from $[Cu(NH_3)_4(H_2O)_2]^{2+}$), NH_3 gas	350 °C, 2 h, NH_3 flow rate: 15 l h^{-1}	irregular particles encapsulated in SiO_2 spheres	15	< 50	[65]
	Cu_2O, NH_3 gas	250 °C, 21 h, NH_3 flow rate: 60 ml min^{-1}	aggregated spheroidal particles	15	22 ± 7	[66]
Solution-based synthesis	$Cu(NO_3)_2$, KNH_2, NH_3 liquid	160 °C, rapid reaction				[69]
	$[Cu(NH_3)_4](NO_3)_2$, Cu, NH_3 liquid	350–580 °C, 600 MPa				[70]
	$Cu(hfac)_2$, NH_3 liquid	200 °C, 16 MPa	cubes		10,000	[74]
	$CuCl_2$, NaN_3, solvent: THF or toluene	1. ~50 °C, 4 h 2. ~100 °C, 10–12 h 3. temperature increase over several days: ~40 °C/day for toluene; ~25 °C/day for THF	fused mass of large aggregates (THF), irregular particles with distorted cubes (toluene)		~50 (toluene) N/D (THF)	[23]
	$Cu(NO_3)_2{\cdot}3H_2O$, ODA	220 °C, 20 min 220–240 °C, 10 min 260–240 °C, 10 min 280 °C, 5 min	spherical particles slightly resembling cubes		50 15 15 10	[77]
	$Cu(NO_3)_2{\cdot}3H_2O$, ODA (or HAD or OAm) + ODE	1. 150 °C, 3 h, 2. 250 °C, 0.5 h	uniform cubes		26 (ODA) 19 (HAD) 11 (OAm)	[55]
	$Cu(NO_3)_2{\cdot}3H_2O$, ODA + OAm	1. 110 °C, 1 h, 2. 240 °C, 10 min	uniform cubes		~25	[78]
	$Cu(NO_3)_2{\cdot}3H_2O$, ODA + OAm	1. 150 °C, 1 h, 2. 230–260 °C, 0.5 h	spherical particles (230 °C) uniform cubes (240–260 °C)		20 (230 °C) 25 (240 °C) 20 (250 °C) 10 (260 °C)	[79]
	$Cu(NO_3)_2{\cdot}3H_2O$, OAm + ODE	1. 110 °C, 0.5 h, 2. 210 °C, 15 min	distorted cubes		10 ± 5	[80]
	PPC, ODA	1. 105 °C, 1 h 2. 260 °C, 5 min.	spherical particles		2.8 ± 0.6	[81]
	$Cu(NO_3)_2{\cdot}3H_2O$, HDA	1. 110 °C, 1 h, 2. 230 °C, 5 min	spherical nanocrystals		4.2 ± 3.2	[82]
	$Cu(NO_3)_2{\cdot}3H_2O$, ODA	1. 115 °C, 1 h, 2. 240 °C, 15 min	uniform cubes	~99	41	[83]
	$Cu(OMe)_2$, benzylamine	80–180 °C, 5–60 min	spherical particles	< 3	< 3	[58,86]
	$Cu(NO_3)_2{\cdot}5H_2O$, HMT, n-hexanol	200 °C, 1 h	quasi-spherical particles		80	[87]
	$Cu(OAc)_2{\cdot}H_2O$, NH_3 gas, $C_nH_{2n+1}OH$ (n = 5–9)	130–200 °C, 1 h NH_3 flow rate: 100 ml/min	aggregates of distorted cubes	< 30	< 300	[56]
	$Cu(OAc)_2{\cdot}H_2O$, $CO(NH_2)_2$, 1-nonanol	190 °C, 1 h 1–10 Eq of $CO(NH_2)_2$	aggregates of distorted cubes (5–10 Eq) spherical particles (1–2 Eq)		100 (10 Eq) 150 (5 Eq) 300 (1–2 Eq)	[88]
	$(C_nH_{2n+1}COO)_2Cu$ (n = 1,2,5,7,9,11,13) NH_3 gas, 1-nonanol	190 °C, 40 min NH_3 flow rate: 100 ml/min	aggregates of distorted cubes, $n \leq 2$ clusters of platelets, $n \geq 5$		~200, $n \leq 2$ < 40, $n \geq 5$	[89]
	CuI, pyridine, NH_3aq, KNH_2	1. −35 °C 2. 130 °C, 30 min	spherical particles	4.2	4.2 ± 0.7	[90]
	CuO, NH_3aq, MeOH	250 °C, 12 MPa, 30 min	pyramidal microcrystals growing from cubic crystalline faces		3000–5000	[91]
	$Cu_2CO_3(OH)_2$ or $Cu(OH)_2$, NH_4OH - NH_4HCO_3	drying 35–200 °C pyrolysis 100–400 °C	porous particles (foams)		~ 1000	[92]
Solid-state synthesis	Cu_2O, $CO(NH_2)_2$	190 °C, 6 h	irregular shape	22	< 500	[66]
	$Cu(OAc)_2$, $CO(NH_2)_2$	300 °C, 2 h	distorted cubes		60–100	[93]
	CuO, $NaNH_2$	150–170 °C, 12–60 h	ill-shaped particles		< 1000	[85]

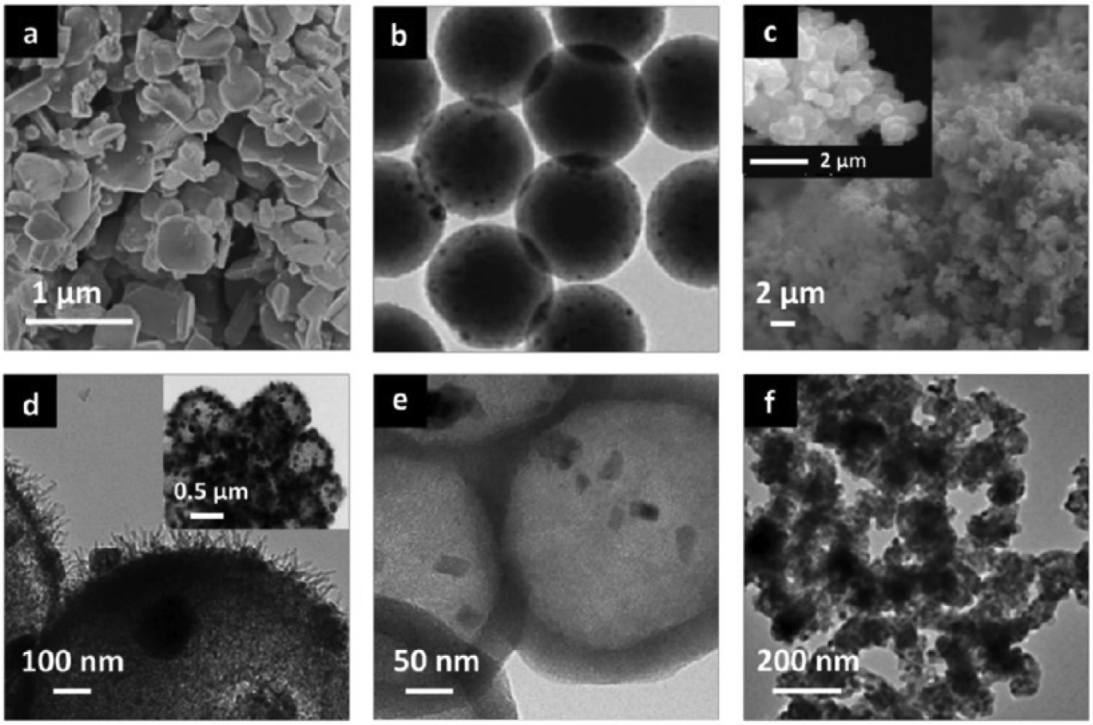

Fig. 2. SEM (a, c) and TEM (b, d, e, f) images of different Cu_3N structures synthesized via ammonolysis: (a) plate-like Cu_3N submicron particles obtained from a CuF_2 precursor [24]; (b) Cu_3N particles supported on silica microspheres from $Cu(OAc)_2{\cdot}H_2O$ [63]; (c) spherical Cu_3N particles obtained from $Cu(CF_3COO)_2$ [64], (d) Cu_3N particles aggregated on the silica surface obtained from $CuSiO_3$ [65], (e) Cu_3N particles encapsulated in silica microspheres from CuO [65]; (f) Cu_2O-derived Cu_3N particles [66]. The figure was reproduced from Ref. [24,63-66] with permission from the rightsholders.

sis of the $Cu(OPiv)_2$ precursor was studied at various temperatures from 180 to 300 °C in order to optimize the reaction process, and pure-phase Cu_3N nanoparticles of ~ 20 nm diameter were obtained by heating at 250 °C for 10 h. In both cases, combustion analysis indicated that the ammonolysis products contained 6.6% N and 6.5% N when using the copper(II) fluoride and copper(II) pivalate precursor, respectively (as compared with a theoretical value of 6.8% N for Cu_3N). The small disparity between the experimental N contents and the theoretical value was within an estimated measurement error level of around ± 0.30%. Moreover, no carbon or hydrogen were detected [67]. Szczęsny *et al.* described preparation of submicron Cu_3N particles (Fig. 2c) using copper trifluoroacetate ($Cu(CF_3COO)_2$) heated under ammonia in a horizontal tube furnace between 250 and 350 °C over durations of 45 min to 5 h. Single-phase Cu_3N was obtained only in the very narrow temperature range 300–310 °C. The progress of the ammonolysis reaction was monitored *in situ* by FTIR spectroscopy and it was indicated that at lower temperatures the reaction was not complete according to the presence of COO, CF_3, NH and CNN bands [64]. Deshmukh and Schubert studied Cu_3N nanoparticles, aggregated on the surface of silica spheres (Fig. 2d), obtained by nitridation of a $CuSiO_3$ precursor at 350 °C for 1 h [65]. The same authors suggested that binary copper oxides themselves could also be used successfully as precursors in ammonolysis reactions. They obtained Cu_3N nanoparticles (size < 30 nm) encapsulated within hollow silica spheres ($Cu_3N@SiO_2$) (Fig. 2e) by starting from copper(II) oxide composite ($CuO@SiO_2$). In this case, the CuO nanoparticles were first obtained in a separate stage from a $Cu(NO_3)_2$ or $[Cu(NH_3)_4(H_2O)_2]^{2+}$ precursor which was adsorbed on a surface of carbon spheres (CS) and coated with a silica shell. The calcination of the as-synthesized Cu(II) precursor/CS/SiO_2 composite led to the selective decomposition of the carbon sphere, and CuO nanoparticles contained within the silica spheres were formed. Ammonolysis of the composite was subsequently performed at 300 °C (10 h) or at 350 °C for 2 h, respectively driving the formation of Cu_3N inside the SiO_2 spheres (a scheme of the synthesis process is presented in Fig. 3) [65].

In a different variation of the oxide precursor ammonolysis experiment, Reichert *et al.* heated copper(I) oxide (Cu_2O) nanocrystals under ammonia at 250 °C for 21 h and obtained spheroidal Cu_3N nanocrystals of 22 ± 7 nm size (Fig. 2f). However, the authors discovered that under these conditions the contamination of the product with some residues of unreacted Cu_2O (6%) was inevitable [66]. Similarly, it is not impossible to consider using Cu(0) as an ammonolysis precursor, but the outcomes appear to be less controllable. As with many other precursors, the temperature band for nitride synthesis appears to be extremely narrow, with copper nitride formation and decomposition competing at temperatures high enough for ammonolysis to occur; the decomposition rate is almost always greater [68].

The ammonolysis reaction is therefore a very versatile way to prepare nitride crystallites of various size - from micro- to nanometers and these dimensions can often be controlled by temperature, ammonia flow rate and reaction time. The technique can be used to produce both unsupported and supported powders with relevance in catalysis. As shown in Fig. 2, nanoparticles of Cu_3N can be deposited *in situ* on substrate surfaces or encapsulated to form different types of nanocomposites (for example, with silica). There is therefore plenty of scope for ammonolysis reactions in the fabrication of a host of new copper nitride-based (or indeed other metal nitride-based) materials, with prescribed dimensions and shapes. Such parameters can indeed be vital for the surface-driven processes that are important in gas sorption or catalysis. There is evidently a large selection of viable copper precursors that can be utilised for ammonolysis reactions, with the most common being Cu(II) salts, oxides or carboxylates. Carboxylates are especially

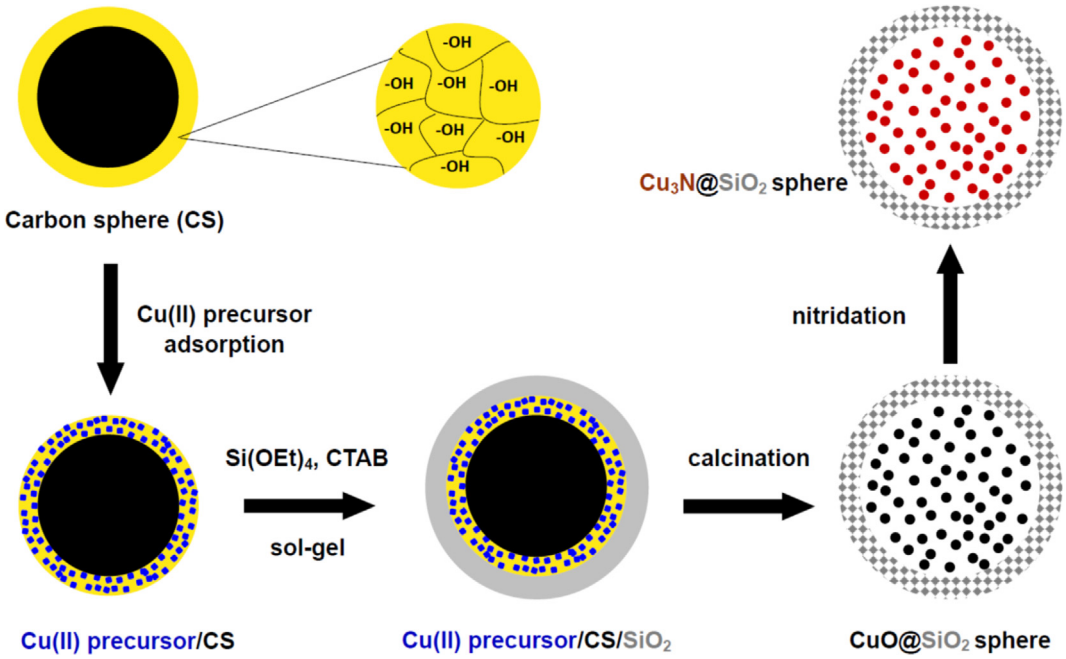

Fig. 3. Schematic showing the multistep synthesis process that yields Cu_3N nanoparticles contained inside hollow mesoporous silica spheres. The figure was reproduced from Ref. [65] with permission from the rightsholder.

promising due to their relatively low stability above 200 °C. The repeatability of ammonolysis and the possibilities of scaling up are also clear advantages of this method.

2.1.2. Solution-based synthesis

The earliest accounts of the solution-based synthesis of Cu_3N originate from 1912, when Edward C. Franklin described the isolation of "ammonated" copper nitride ($Cu_3N{\cdot}nNH_3$) from the reaction of potassium amide (KNH_2) with a liquid ammonia solution of copper(II) nitrate. Heating the obtained precipitate at 160 ℃ led to the formation of black Cu_3N powder [69]. A solution-based synthesis of copper nitride was not reported subsequently until 1990 when Zachwieja and Jacobs described a solvothermal method leading to the growth of Cu_3N crystals via the reaction of $[Cu(NH_3)_4](NO_3)_2$ with Cu in liquid ammonia. Further heating of either the tri- or di-amine copper(I) nitrate ($[Cu(NH_3)_x]NO_3$, $2 \leq x \leq 3$) between 350 and 580 °C range under 600 MPa of NH_3 resulted in decomposition to copper nitride, nitrogen and water [70] (Eq. (1)).

$$3\,[Cu(NH_3)_n]NO_3 \rightarrow Cu_3N + 9\,H_2O + 4\,N_2 + (3n\text{-}6)\,NH_3 \quad (1)$$

The Jacobs and Zachwieja method was denoted "ammonothermal" synthesis to describe a solvothermal method analogous to the hydrothermal methods used with water as a solvent. The method has since been widely adopted in the synthesis of metal nitrides. In the most general sense, solvothermal synthesis is usually defined as a reaction in a solvent, in which the reaction mixture is heated above the solvent boiling point at a pressure exceeding 1 atm. The synthesis is performed in a sealed reaction vessel (stainless steel autoclave) due to the autogenous pressure that develops during the progress of the reaction [71]. In practice, ammonothermal synthesis is performed at near-critical or supercritical conditions (T_C = 132 °C, P_C = 11.3 MPa for ammonia) [72,73]. An adapted ammonothermal method has since been employed to grow cubic Cu_3N monocrystals (~10 μm in size) from a $Cu(hfac)_2$ precursor at 200 °C and 16 MPa. The modification to the experiment involved the use of methanol as a cosolvent (molar ratio NH_3:CH_3OH = 7:3) to improve the precursor solubility and to decrease the onset temperature of decomposition [74].

The main advantages of the solvothermal method are the simplicity of a single-step synthesis approach and the removal of post-synthesis thermal treatments to achieve highly crystalline products [75]. Solvothermal synthesis enables otherwise-impossible metathesis reactions to be performed to yield metastable transition metal nitrides. The highly exothermic conditions of solid-state metathesis would preclude the formation of such compounds [76]. The true power and versatility of solvothermal techniques, however, was revealed later by Choi and Gillan, who demonstrated that the method could be tuned from one of single crystal growth to one of nanoparticle production. Nanocrystalline Cu_3N was obtained via solvothermal synthesis using either THF or toluene as a solvent and occurs through the *in situ* thermal decomposition of copper azide ($Cu(N_3)_2$). A $CuCl_2$ precursor was reacted with NaN_3 in toluene or THF (Eq. (2)) in an argon-filled stainless steel reactor by heating to ~ 50 °C for 4 h and to ~ 100 °C for 10–12 h (ensuring a maximum reaction temperature of 140 °C for toluene and 120 °C for THF). By then slowly increasing the reaction temperature to 185 °C for 1 day the initially formed copper azide was thermally decomposed to Cu_3N (Eq. (3)). When using THF, the resulting nitride product in the form of a fused mass was composed of large aggregates of microstructures, with irregular empty spaces. If THF is replaced by toluene as the solvent in the reaction, then fine powders consisting of well-defined structures with some slightly distorted nanocubes (~50 nm across), of higher crystallinity and purity are formed [23].

$$CuCl_2 + 2\,NaN_3 \rightarrow Cu(N_3)_2 + 2\,NaCl \quad (2)$$

$$Cu(N_3)_2 \rightarrow CuN_x + (3\text{—}0.5x)\,N_2 \quad (3)$$

The use of non-aqueous solvents in the synthesis of nitrides continued to pique the interest of researchers in the following years, who were enticed by the opportunity to control the size and shape of such materials for the first time. The thermal decomposition of copper salt precursors in long-chain amines or alcohols quickly became a much-used technique. Wang and Li obtained pure, single-crystalline Cu_3N nanocubes with sides of 15 nm by the thermal decomposition of $Cu(NO_3)_2{\cdot}3H_2O$ at 240 °C in 1-

octadecylamine (ODA) at atmospheric pressure [77]. It was suggested that ODA plays a key role in the shape-selective process with a function similar to a catalyst. The long-chain amine modifies the decomposition routes of $Cu(NO_3)_2$ as compared to the equivalent solid state process or to decomposition reactions performed in solution formed with other solvents (Eqs. (4) and (5)). ODA is proposed to offer electrons to Cu^{2+} and N^{5+} to facilitate reduction but the amine is not hypothesised to participate in the reaction as a nitrogen source. To confirm this viewpoint, authors used other copper salts ($Cu(OAc)_2$, $CuCl_2$, or $CuSO_4$) and results demonstrated that Cu_3N was not obtained.

$$2\ Cu(NO_3)_2 \rightarrow 2\ CuO + 4\ NO_2 + O_2\ (\textit{solid state reaction}) \quad (4)$$

$$3\ Cu(NO_3)_2 \rightarrow Cu_3N + 5\ NO_2 + 4\ O_2\ (\textit{reaction in ODA}) \quad (5)$$

Size and morphology control can be exerted by variation of the synthesis conditions, for example, increasing the temperature from 220 °C to 280 °C resulted in the reduction of the particle size from 50 nm to 10 nm. Moreover, the phase composition of the products could be modified through the $Cu(NO_3)_2$:ODA molar ratio and single-phase nitride was obtained only at a ratio of 3:80, which appears to be sufficient to exceed the potential barrier of reaction (5) and Cu^{2+} and N^{5+} can be co-reduced. Changing the $Cu(NO_3)_2$: ODA ratio resulted in the formation of Cu and Cu_2O nanocrystals with or without Cu_3N. Wu and Chen also synthesized Cu_3N nanocubes (NCs), each 26 nm across, from copper(II) nitrate using a mixture of 1-octadecylamine and 1-octadecene (ODA/ODE) (volume ratio 1:1) [55]. The degassed solution was heated at 150 °C for more than 3 h and further at 250 °C for 30 min. The authors related the formation of the cubic nanocrystals to the binding of ODA at the (1 0 0) faces of Cu_3N, which in turn retarded the growth of the crystals in that direction. The primary amines therefore likely act as both solvents and capping agents in this reaction. In addition, if a different selection of amine reagent is made then it becomes possible to influence the size of the nanocubes. Reaction with hexadecylamine (HAD) or oleylamine (OAm), instead of ODA, resulted in the formation of nanocubes with sides of 19 nm or 11 nm, respectively. The discovery of these relatively simple and controllable methods of Cu_3N nanocube syntheses led to further subsequent studies in which either other reagents were investigated specifically to engineer cubes of different sizes or in which the synthesis routes could be modified to create nanocomposites of increased compositional and structural complexity. Employing different solvent mixtures, reaction temperatures and reaction times could all have profound effects on the size and/or morphology of the product. For example, Xi *et al.* obtained nanocubes that were ~ 25 nm across (Fig. 4a) utilizing again $Cu(NO_3)_2{\cdot}3H_2O$ as a copper precursor, which was dissolved in a mixture of ODA with OAm solvents, followed by degassing at 110 °C for 1 h and heating at 240 °C for only 10 min [78]. A three-stage mechanism was proposed to describe the growth of the nanocubes: (i) nucleation to form nanoparticles; (ii) growth of the nanoparticles to form nanocubes as a result of the surface tension effects of the solvents and finally, (iii) a "molding stage" which leads to homogeneously dispersed uniform nanocubes. Yin *et al.* synthesized Cu_3N nanocubes, in an ODA/OAm mixture (~1:0.8 mass ratio), with side dimensions of 25, 20 and 10 nm respectively by heating at either 240, 250 or 260 °C (for 30 min in each case) [79]. It was suggested that a higher processing temperature promotes faster nucleation and results in smaller NCs. Moreover, cubic-like nanostructures require a reaction temperature of at least 240 °C, whereas at 230 °C spherical nanoparticles are formed. Barman *et al.* succeeded in obtaining nanocubes that were 10 ± 5 nm across using an OAm/ODE solvent mixture (1:1 vol ratio) at 210 °C for 15 min [80]. These small nanocubes were then decorated by gold nanoparticles using thermal- or light-induced growth processes. In the first case, the Au stock solution, prepared from chloroauric acid dissolved in OAm/ODE mixture solution, was added to a Cu_3N dispersion in ODE. The final mixture was heated at 50 °C for 10 min and Au-Cu_3N heterostructures with Au NPs with an average size of ~ 5 nm were obtained. Decoration via a light-induced process was performed by the addition of a sonicated transparent Au solution (chloroauric acid dissolved in OAm) to Cu_3N dispersion (prepared analogously as in the thermal process) followed by stirring upon light irradiation for 4 h. After that the mixture was heated at 40 °C for 15 min. As a result, single Au NPs with an average size of ~ 10 nm were decorated on particular corners of the Cu_3N structures. Therefore, light-induced thermal growth promotes selective Au NPs deposition. The authors explored optical properties and photocatalytic activity towards methylene blue and methyl orange. The Au-Cu_3N heterostructures exhibit enhanced catalytic activity in comparison to pure Cu_3N nanocubes.

A modified synthetic approach was presented by Sithole and co-authors. They prepared copper nitride nanocrystals using a bis(pyr role-2-carbalpropylominato) (PPC) Cu(II) complex as a precursor and employed only ODA as a solvent. After degassing the solution at 105 °C, for 1 h, followed by very brief heating at 260 °C for 5 min, it was observed that the resulting Cu_3N nanocrystals were spherical in stark contrast to the nanocubes that form almost by default when using a copper nitrate precursor [81]. The authors concluded that the pre-existing Cu–N bond in the PPC complex starting material prevents the formation of either CuO or Cu among the reaction products and that, by analogy, the use of precursors containing NO_3^- also act as nitrogen sources and similarly prevent the formation of oxide products. It was not obvious from these data alone, however, as to why spheres were formed using the PPC precursor. Some of the same authors then also studied the effects of returning to $Cu(NO_3)_2{\cdot}3H_2O$ as a precursor and contrasting ODA with HAD as solvents in the Cu_3N synthesis. The ODA and HAD solvent reactions led to 41 nm sided nanocubes and 4 nm diameter spherical particles, respectively. It was also found that the synthesised Cu_3N NCs could be easily sulfided to form Cu_2S and Cu_9S_5 [82,83].

The latest research in this field has focused on the effect of time on the synthesis of Cu_3N nanoparticles in octadecylamine (ODA) [84]. Copper(II) nitrate was used in these experiments as a precursor and thermally decomposed at 260 °C. The authors proposed that four steps were involved in the nitrate thermolysis: nucleation, growth, ripening and decomposition. After maintaining the temperature for 15 min, well-defined copper nitride particles with a size of 39 ± 8.4 nm were obtained. Increasing the time to 20 min induced the disintegration of the cubes and all the copper nitride decomposed to metallic copper within 60 min. In contrast to the earlier proposed role of ODA, the authors suppose that the amine acively participates in the reaction. The presence of a nitrile (RCN) as a product of the thermal decomposition of octadecylamine and, possibly, a capping agent of Cu_3N particles was consistent with the results of FTIR and NMR spectrum analyses, and the following reaction was proposed (Eq. (6)):

$$3\ Cu(NO_3)_2 + 3\ CH_3(CH_2)_{16}CH_2NH_2 \rightarrow Cu_3N + 5\ NO + 7/2\ O_2 + 6\ H_2O + 3\ CH_3(CH_2)_{16}C{\equiv}N \quad (6)$$

From the various solvothermal syntheses reported above, a perceived disadvantage of the procedures using long-chain amines such as ODA and OAm would be the requirement for reaction temperatures above 200 °C. This issue was overcome by Deskmukh *et al.* who discovered that the fabrication of ultrasmall (~2 nm) Cu_3N particles (Fig. 4b) could be achieved by the reaction of a copper(II) methoxide ($Cu(OMe)_2$) precursor with benzylamine (under argon) at lower temperatures for short reaction times (e.g. 140 °C for 15 min). The reaction mechanism for the Cu_3N synthesis that was proposed by the authors is presented below (Eqs. (7)–(10)).

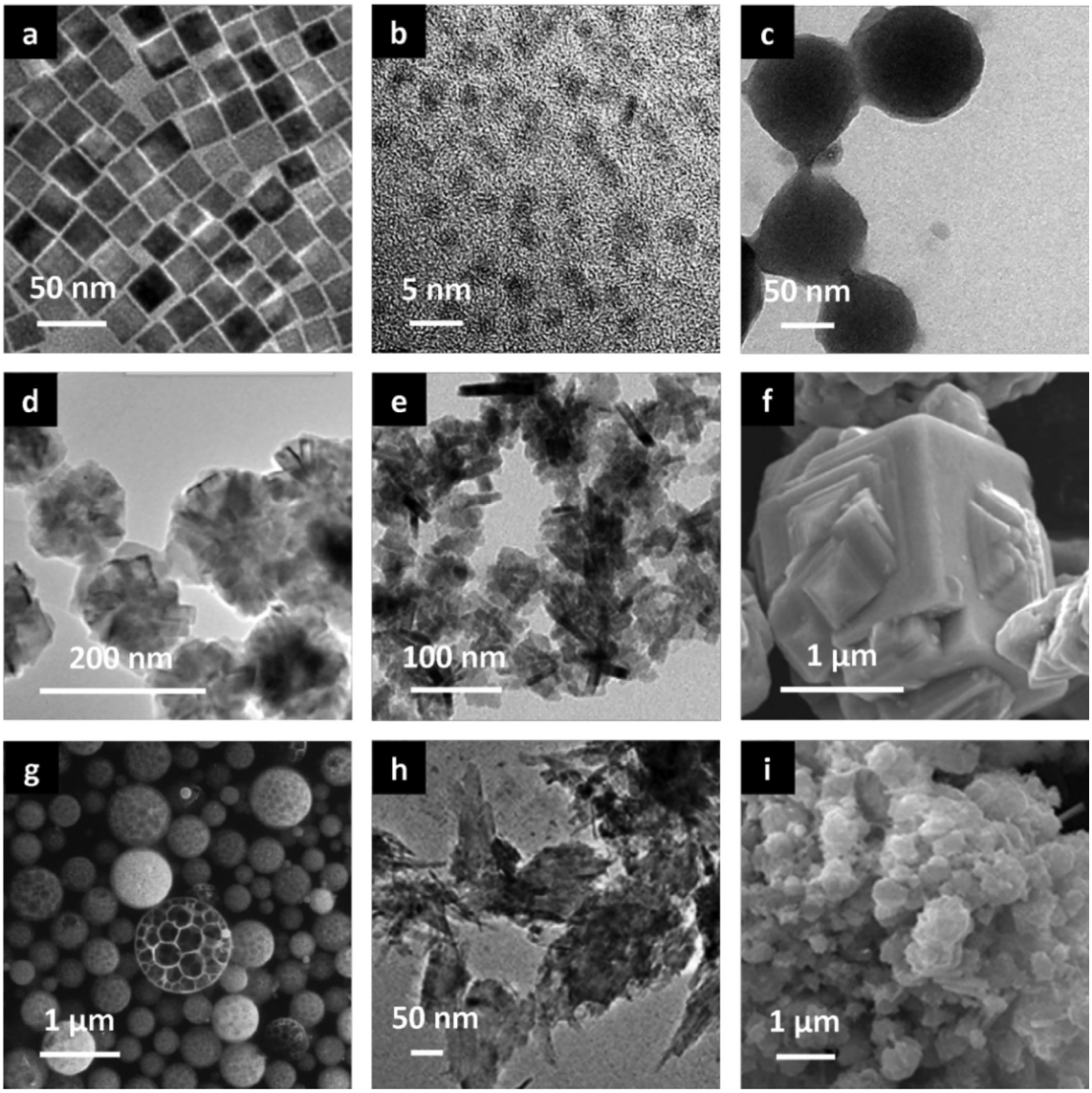

Fig. 4. SEM (f, g, i) and TEM (a-e, h) images of different Cu_3N structures synthesized via solution-based (a-g) and solid-state (h-i) synthesis showing: (a) an ordered array of Cu_3N uniform nanocubes from $Cu(NO_3)_2{\cdot}3H_2O$, precursor in ODA/OAm [78]; (b) spherical particles from $Cu(OMe)_2$ precursor and benzylamine [58]; (c) quasi-spherical particles from $Cu(NO_3)_2{\cdot}5H_2O$ precursor and HMT/n-hexanol [87]; (d) aggregates of distorted cubes from $Cu(OAc)_2{\cdot}H_2O$ precursor with NH_3 gas and 1-nonanol [56]; (e) clusters of platelets synthesized from a copper tetradecanoate precursor with NH_3 gas and 1-nonanol [89]; (f) pyramidal microcrystals growing from cubic crystalline faces formed in the reacion of CuO, NH_3aq and MeOH (SEM image) [91]; (g) porous microparticles (foams) synthesised from a $Cu_2CO_3(OH)_2$ precursor and NH_4OH - NH_4HCO_3 solution [92]; (h) irregular nanocrystals produced from Cu_2O and urea [66], and (i) ill-shaped submicron particles from the solid state reaction of CuO with $NaNH_2$ (SEM image) [85]. The figure was reproduced from Ref. [56,58,66,78,85,87,89,91,92] with permission from the rightsholders.

Altering the reaction temperature and time had somewhat predictable effects on the average crystallite size; crystallites increased from 1.8 to 2.8 nm across as the temperature was increased from 80 °C to 180 °C (reaction time was 1 h in each experiment), whereas upon extension of the reaction time from 5 to 60 min (at 140 °C), the crystallite size increased from 2.2 to 2.5 nm accompanied by a more uniform size distribution. FT-IR and TEM studies indicated that the benzylamine modifies the surface of nanoparticles and plays the role of a surfactant that prevents NP agglomeration [58].

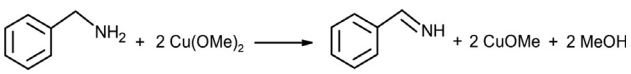

(7)

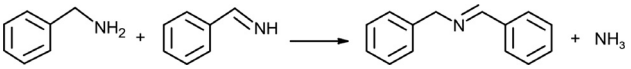

(8)

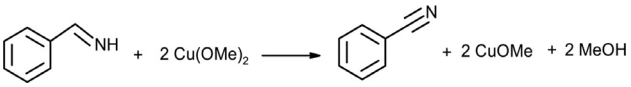

(9)

$$3\ CuOMe + NH_3 \rightarrow Cu_3N + 3\ MeOH \quad (10)$$

The Cu_3N NPs prepared using benzylamine were subsequently used as a component of the first reported transition metal nitride aerogel in the form of 3D network of ultrasmall nanoparticles

bridges. The specific surface area of the nitride aerogel was determined to 381 $m^2\ g^{-1}$, which is almost 40 times greater than that of bulk Cu_3N powder (10 $m^2\ g^{-1}$) and significantly higher than reported value for Cu_3N nanostructures (48 $m^2\ g^{-1}$) [85]. The average density of the aerogel was calculated to be 0.31 g cm^{-3}, which makes this value about 20 times lower than that of the bulk powder (5.84 g cm^{-3}). Such highly porous Cu_3N-based materials, showing extremely different properties from the corresponding bulk powders, can be used for improved applications, e.g. in the field of catalysis [86]. Mondal *et al.* reported a solvothermal process realized by using hexamethylenetetramine (HMT), in which the amine acted both as a reducing and nitriding agent, albeit indirectly (Eqs. (11)–(13)). The process involved the dispersal of the precursor $Cu(NO_3)_2{\cdot}5H_2O$ in n-hexanol prior to the addition of HMT. The mixture was purged with argon and heated at 200 °C for 1 h. Three reaction steps were proposed to occur: (i) *in situ* generation of ammonia and formaldehyde, (ii) reduction of Cu(II), and (iii) nitridation of Cu(I) by NH_3 produced *in situ*. Quasi-spherical shaped Cu_3N nanoparticles with an average size of 80 nm were obtained (Fig. 4c) [87].

$$C_6H_{12}N_4 + 6\ H_2O \rightarrow 6\ HCHO + 4\ NH_3 \quad (11)$$

$$2\ Cu^{2+} + HCHO + H_2O \rightarrow 2\ Cu^{+} + HCOOH + 2H^{+} \quad (12)$$

$$3\ Cu^{+} + NH_3 \rightarrow Cu_3N + 3H^{+} \quad (13)$$

Nakamura *et al.* demonstrated that amines could be replaced by long-chain alcohols and ammonia in the synthesis of Cu_3N nanoparticles from a suitable copper precursor (in this case, copper(II) acetate monohydrate; Fig. 4d). Ammonia gas (100 ml min^{-1}) was fed into solutions formed from long-chain alcohols ranging from 1-pentanol to 1-nonanol heated from 130 °C to temperatures close to the respective solvent boiling points (~200 °C). Single-phase Cu_3N was obtained only in 1-nonanol, 1-octanol or 1-heptanol. It was observed that the purity of the nitride product was improved with increasing alkyl chain length, thus the increased hydrophobicity of the solvent and at higher temperature, thus eliminating water from the reaction mixture [56]. The authors proposed three stages in the mechanism of the nitridation reaction on the basis of visual assessment of the solution color, UV–Vis spectroscopy measurements, and GC–MS analysis of the supernatant solution after Cu_3N synthesis. They explicitly evoked the formation of an ammine complex in the first step, viz. (i) the formation of the copper(II) ammine complex by reaction with ammonia; (ii) the reduction of the Cu^{2+} centre to Cu^{+} by the long-chain alcohol; (iii) decomposition of the ammine complex under ammonia to form the nitride (Scheme 1).

Urea ($CO(NH_2)_2$) was proposed as a more environmentally friendly source of active nitrogen than ammonia. Nakamura and co-workers showed that the composition, size and morphology of the product could be controlled by varying the molar ratio of urea to the copper-containing precursor ($Cu(CH_3COO)_2{\cdot}H_2O$) [88]. Pure copper nitride was obtained in the form of fairly large nanoparticles (ca. 150 nm across) when at least 5 equivalents of urea were used (5:1 urea:copper salt). By contrast, two or fewer urea equivalents resulted in copper(I) oxide formation. Nakamura went on to

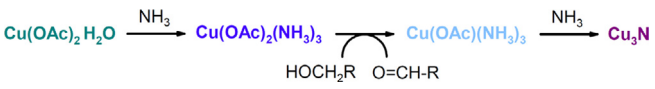

Scheme 1. The proposed reaction mechanism of copper nitride formation using long chain alcohols and ammonia. (The font color corresponds to the colors of the solutions.) The figure was reproduced from Ref. [89] with permission from the rightsholder.

demonstrate that varying chain length fatty acids could be integrated within the salt precursor itself to produce Cu_3N nanoparticles of varying morphology [89]. Using a series of fatty acid copper (II) salts ($(C_nH_{2n+1}COO)_2Cu$; where n = 1, 2 ,5 ,7 ,9 ,11 and 13) as precursors, anisotropic plate-like particles were formed for $n \geq 5$ (Fig. 4e), while for shorter chain lengths, approximately isotropic spherical particles were obtained [89].

Alternatives to "standard" solvothermal syntheses demonstrated that Cu_3N could also be synthesized under relatively extreme conditions, despite its metastable nature. Egeberg *et al.* [90] developed an oxygen-free synthesis of Cu_3N nanoparticles at low-temperature, using pyridine as a solvent and copper(I) iodide as a precursor. In this approach, liquid ammonia and KNH_2 were added to a starting solution of CuI in pyridine at −35 °C, resulting in formation of a copper(I) amide, $Cu(NH_2)$. The amide could then be refluxed in pyridine at 130 °C to yield single phase Cu_3N spherical nanocrystallites (size ca. 4 nm) [90]. A radically different approach was adopted by Li *et al.* who succeeded in growing Cu_3N pyramidal microcrystals (Fig. 4f) by heating a copper oxide (CuO) precursor in a mixture of supercritical methanol and ammonia over a temperature range of 200–280 °C under a self-generated pressure of between 9 and 14 MPa [91]. Pure-phase Cu_3N was achieved at 250 °C and 12 MPa and it was suggested that MeOH acts not only as a solvent but also as a reducing agent under supercritical conditions.

An even more unconventional variation of a solution-based Cu_3N synthesis was developed by Kieda and Messing who applied a spray pyrolysis technique using copper-ammine complex solutions [92]. The precursor solutions were prepared by dissolving $Cu_2CO_3(OH)_2$ or $Cu(OH)_2$ in NH_4OH - NH_4HCO_3 solutions, which were then passed into a tube furnace as an aerosol using an ultrasonic nebulizer. A single-phase Cu_3N product could be obtained when using a $Cu(OH)_2$ precursor in 1 M NH_4HCO_3 solution, which after nebulization was dried at 100 °C and subjected to pyrolysis at 400 °C. However, it was not possible to obtain a pure nitride product when using a $Cu_2CO_3(OH)_2$ precursor and multi-phase powders composed of CuO, Cu_2O and Cu_3N resulted (Fig. 4g).

From the evidence presented in this section, the solution-based synthesis of copper nitride (Fig. 4) can present several advantages in comparison to the ammonolysis of a solid copper precursor by ammonia gas: (i) it is possible for solution reactions to be performed at lower temperature (usually at elevated, autogenerated pressure) with the main limiting factor being the boiling temperature of the solvent; (ii) it is not unusual to produce single-phase product with appropriate choice of precursor and solvent; (iii) solvents themselves (such as long chain amines) can be employed as the nitrogen source, often fulfilling principles of green chemistry; (iv) the temperature of the reaction can be used to control the size and shape of Cu_3N crystallites and can be exploited to particularly favour nanoparticle formation; (v) the use of non-gaseous nitrogen sources as starting materials (such as amines or urea) ensures easy handling and higher precision in controlling the molarity of the reagents, which is crucial for the quality of the product; (vi) there is considerable flexibility in the available choice of copper precursors from simple salts through hydroxides and oxides, to Cu(II) complexes and chelates. The only restriction appears to the oxidation state of the copper in the precursor; in all reported cases except one (when a Cu(I) precursor was utilized), suitable precursors have contained copper(II) ions and one electron reduction has proved to be an important step in the synthesis process.

There would still appear to be a large number of chemical tools available towards the ambition of producing copper nitride of controlled size and shape reproducibly and in sizeable quantities. From the many solution synthesis studies already performed, it is evident that degrees of Cu_3N synthesis control can be exerted by physical parameters such temperature and pressure and by chem-

ical variables such as solvent, nitrogen source, and precursor selection.

2.1.3. Solid state synthesis

While by no means as widespread as solution or solid–gas techniques, methods have also been reported to prepare copper nitride exclusively in the solid state. Reichert *et al.* [66] successfully synthesized Cu_3N (Fig. 4h) by nitridation of Cu_2O nanocrystals with urea in a steel autoclave at 190 °C for 6 h. The study determined that the solid state reaction with urea instead of reaction with gaseous ammonia used by authors as a second nitrogen source (see 2.1.1.), resulted in improved phase purity of Cu_3N leaving only 1.6% Cu_2O and 0.4% CuO as contaminants [66]. In 2019 Panda *et. al.* developed another angle to urea-based Cu_3N synthesis which incorporated aspects of both solid state synthesis and gas–solid reactions (ammonolysis). In their experimental set up, a solid copper(II) acetate precursor was placed downstream from solid urea in a tube furnace operating with a flow of Argon gas (2–3 l h^{-1}). The advantages of this arrangement, as opposed to the use of NH_3 gas, come from the easy handling of urea and the ability to prevent the over-reduction of the precursor to metallic copper in a controlled manner. On heating (at 300 °C for 2 h), liberated ammonia (from urea decomposition) reacts with the copper precursor to produce phase-pure nanocubes (60–100 nm across), which were subsequently deposited on either nickel foam or fluoride-doped tin oxide as electrodes for water electrolysis studies in alkaline media [93].

Aside from urea, amides could prove to be a reactive alternative solid state nitrogen source, but studies have to-date been very limited. Miura *et al.* were able to prepare sub-micron Cu_3N particles by the solid-state reaction of the oxide precursor, CuO and sodium amide, $NaNH_2$. Heating the powders under nitrogen at temperatures of 120–190 °C over periods between 12 and 60 h was successful in producing the required nitride product (Eq. (14); Fig. 4i). Single-phase Cu_3N formation was possible over the narrower temperature range of 150–170 °C when heated for 60 h [85].

$$3\ CuO + 3\ NaNH_2 \rightarrow Cu_3N + 3\ NaOH + NH_3 + 1/2\ N_2 \qquad (14)$$

Solid state synthesis methods to Cu_3N remain relatively untested and have been performed almost exclusively with urea as a nitrogen source. It is unclear whether the reaction proceeds by the initial thermal decomposition of urea in all these cases. The copper precursors in these reactions need be no different from those used in solid–gas or solution state syntheses and just as in the latter case, the particle size appears to be controllable as a function of reaction temperature and time. In principle, however, the range of solid nitrogen sources extends significantly beyond urea (and sodium amide) and their successful selection is likely to be governed by their relative stability; highly exothermic reactions will undoubtedly lead to Cu_3N decomposition and has previously excluded the use of solid state metathesis techniques to synthesise metastable late transition metal nitrides using alkali or alkaline earth metal nitrides for example [94].

2.2. Thin films of copper nitride

Methods to prepare transition metal nitride thin films can be divided essentially into physical and chemical approaches [95]. Among these fabrication techniques, the vast majority can be classified under the category of physical deposition methods (PVD), which mostly comprise RF or DC magnetron sputtering techniques, but also include molecular beam epitaxy (MBE), pulsed laser deposition (PLD) and ion-assisted deposition (IAD). By contrast, the number of different Cu_3N chemical deposition methods that have been described is rather more limited and approaches are dominated by variations on chemical vapor deposition (CVD) or ammonolysis reactions (AR) for this purpose. In this following section, the requirements of both physical and chemical growth methods will be considered with an emphasis on the latter strategy. The parameters that govern the successful deposition of copper nitride films will be presented and discussed.

2.2.1. Physical deposition methods

When considering the history of Cu_3N thin film studies, it is worth beginning with the research dedicated to the reconstruction of a copper surface exposed to nitrogen. Several experimental studies have been conducted in order to understand the interaction between gaseous nitrogen and the Cu(100), Cu(110) and Cu (111) surfaces [96–100]. Since molecular nitrogen does not readily chemisorb on a copper surface, due to the strong N-N bond, the gas first has to be activated in an electron beam during exposure [101,102]. Lee and Farnsworth reported the first studies on N/Cu (100) interactions using low-energy electron diffraction (LEED) and observed formation of a two dimensional surface Cu(100)c (2x2)-N (i.e., Cu_2N) [101]. Further research on the N-Cu(100) system performed by Burkstrand *et al.* indicated that the nitrogen binds to the surface at a four-fold-hollow (ffh) symmetric site, while adsorbed 0.145 nm above the first layer of copper [103,104]. Deposition of more than a half of a disordered monolayer was performed using a 100 eV beam and a pressure of $5{\cdot}10^{-5}$ Torr, followed by heating at 445 °C, which resulted in layer modification and the formation of an ordered c(2x2) pattern [99]. Zeng *et al.* prepared an ordered Cu(100)c(2x2)-N surface by exposing copper to nitrogen gas activated by a 200 V ion gun at $5{\cdot}10^{-5}$ Torr, and annealed at 270 °C [105]. The detailed study of the reconstructed surface structure was based on a comparative model of bulk copper nitride. Heskett *et al.* suggested that copper nitride layers formed due to the nitrogen-induced reconstruction of the Cu(110) surface into a (2x3) pattern (under an applied pressure of ~ $5{\cdot}10^{-5}$ Torr, using a beam energy of 200 eV and a current of ~ 2 μA) [98]. Also Grimsby *et al.* studied the Cu(110)-(2x3)-N surface formed after nitrogen-ion bombardment (with a beam energy of 200, 250 or 500 eV and a nitrogen pressure of 5-9·10^{-5} Torr) and suggested a model in which every other <001> row is missing and a structure analogous to the Cu_3N(110) surface, where every third nitrogen atom was lacking [106]. Scanning tunneling microscopy (STM) studies of the Cu(100)c(2x2)-N surface ($5{\cdot}10^{-4}$ Torr, 500 eV) revealed formation of square-shaped structures with 5.2 nm sides, running parallel to the [100] directions [97]. In subsequent years, numerous reports in the literature described the structure of the so-formed ultrathin Cu_2N layers or islands also referred to as 'copper nitride', but a detailed description of the different N/Cu adsorption phases will not be discussed in this review, since it has already been the subject of a large number of experimental and theoretical studies [107-109].

Sputtering is well-known among physical vapour deposition (PVD) methods used for the fabrication of films of metals, alloys, oxides, fluorides, carbides and nitrides (among others). Four variations of sputtering are commonly employed: radio-frequency (RF), direct current (DC), magnetron and reactive sputtering [110]. Since the pioneering work by Terada *et al.* (1989) on the epitaxial growth of copper nitride, RF sputtering has become the most widely used mode of copper nitride thin film fabrication. The authors obtained a single crystalline Cu_3N thin film using a Cu metal target and several alternative substrates: (0001)-cut Al_2O_3, MgO, $SrTiO_3$, glass and highly-oriented Pt films epitaxially grown on MgO (Pt/MgO). An argon/nitrogen mixture (Ar:N_2 = 3:2) was used as a sputtering gas at a pressure of 30 mTorr while maintaining a substrate temperature of 100 °C. The highest quality Cu_3N films were grown on Pt/MgO substrates, with a preferred (100) plane orientation [111]. Later, Maya successfully deposited nitride films of tin, cop-

per and nickel by DC reactive sputtering in a nitrogen plasma [41]. The quality of the films was such that the chemical composition and thermal behavior of the Sn_3N_4, Cu_3N and Ni_3N materials could be studied systematically; the crystalline Cu_3N film was discovered to decompose at 465 °C (He; 10 °C min^{-1}), which is significantly higher than the temperature usually observed for bulk powder (see section 2.3). Various other modifications of sputtering techniques have also been successfully employed to fabricate Cu_3N films, including reactive RF magnetron sputtering ion plating (MSIP) [112], DC triode sputtering [48], ion beam assisted DC magnetron sputtering [113] and pulsed magnetron sputtering [96].

From the point where Cu_3N films were first grown, the majority of subsequent physical deposition studies was focused on manipulating the sputtering process conditions to improve the structural properties of the nitride films. In consideration of the thermodynamic metastability of copper nitride, it is the nitrogen activity on the substrate surface that is the factor that determines the growth and physical properties of a Cu_3N film [29]. This, in turn, can be tuned via the sputtering process parameters such as the total gas pressure in the reaction chamber, the nitrogen content in the gas mixture, the substrate temperature and the substrate-target distance; each of these processing variables has been studied in detail. In one such systematic study, Maruyama *et al.* deposited highly [100] oriented polycrystalline Cu_3N films by RF reactive sputtering (RF power: 20–400 W, substrate temperature: 50–300 °C, total sputtering pressure: 0.76–28 mTorr) and noted the correlation of the cubic Cu_3N lattice constant, *a*, with the substrate temperature, total reaction chamber pressure, and the power of the RF source [114].

The nitrogen partial pressure has also proved to be a significant variable in sputtering and can have a considerable impact on the grain size, crystal orientation and stoichiometry of Cu_3N films. These features of the film are critical in determining the optical and electrical properties of the deposited material [39,42,52,115,116]. The composition of copper nitride films was demonstrated to be highly sensitive to the total sputtering pressure (over an applied range of 6.7–130 Pa) and on the N_2 content within the chamber (0–100%) [52]. Four categories of Cu–N films could be defined under these conditions of varying nitrogen partial pressure: (i) metallic Cu-rich films with a positive temperature coefficient of resistivity (TCR), (ii) semiconducting Cu-rich films, (iii) semiconducting stoichiometric Cu_3N films and (iv) semiconducting N-rich films with a negative TCR. The transition from sub-stoichiometric (Cu-rich) phases to the stoichiometric phase was noted at a 75% (minimum) content of nitrogen and a total pressure of 67 Pa (or a 50% nitrogen content at a total pressure of 130 Pa), whereas the change from metallic to semiconducting Cu-rich phases occurred at an N_2 content of 50% at 67 Pa (or 10% N_2 at 130 Pa). Soon afterwards it was observed that the film deposition rate slightly increases for nitrogen partial pressures between 0.03 and 0.13 Pa prior to decreasing again gradually (above 0.13 Pa). Strongly textured films, again with a [100] crystal growth direction, were produced at a temperature of 100 °C, an applied RF power of 100 W and a nitrogen pressure of 0.4 Pa [42].

Other studies focused on the substrate temperature during the deposition process and its impact on the structural, mechanical and opto-electrical properties of copper nitride films [49,117,118]. The microhardness of films can increase from 2.7 to 4.4 GPa by increasing the substrate temperature from 30 to 200 °C, although this declines to 4.1 GPa when the temperature is raised further to 250 °C [49]. Simultaneously, these substrate temperature increases from 30 to 250 °C had the effect of decreasing the electrical resistivity of the films from $8.7{\cdot}10^{-1}$ to $1.1{\cdot}10^{-3}$ Ω cm and narrowing the optical band gap from 1.89 to 1.54 eV. Kim *et al.* noted an important correlation between sputtering conditions and growth showing that film growth in the [111] direction became preferable at N_2 pressures below 2.50 mTorr (at a substrate temperatures of 150 °C), whereas the normal [100] growth direction resumed at 3.75 mTorr (and a substrate temperature of 250 °C) [38].

Perhaps unsurprisingly, just as N_2 partial pressure can have an impact on the composition and structure of copper nitride films, so can the nitrogen flow rate exert a considerable influence and its effect on growth rate, grain size and morphology has been studied extensively [37,119–122]. For example, Pierson *et al.* investigated the sensitivity of RF-sputtered Cu_3N film composition and structure to the nitrogen flow rate and noted that below 4 sccm (cm^3 min^{-1} under standard conditions) the films were sub-stoichiometric, while at higher flow rates they were over-stoichiometric in nitrogen. At the critical nitrogen flow rate of 4 sccm, the layers are almost stoichiometric. The size of the nodular-like grains within the films became larger as the nitrogen flow rate was increased and the usual [100] orientation was observed for N_2 flow rates in excess of 4 sccm. Just as was observed for lower nitrogen partial pressures in earlier studies, the film growth switched to the [111] direction at lower N_2 rates (3–4 sccm) and accordingly the morphology of the film changed to one of a "facetted" (pyramid-like) crystalline appearance [120].

Generally the dominance of sputtering methods in the fabrication of metal nitride thin films arises from the rapid deposition rate, strong adhesion and high quality that can be achieved [123]. Sputtering methods offer versatility and fine control of deposition parameters (e.g. nitrogen partial pressure and flow rate, deposition pressure and temperature, applied RF power), which yield copper nitride films of high specification, repeatably and reliably. Physical deposition methods are likely to be central in the future development of materials based on copper nitride films. This is equally true of evolving physical deposition techniques - such as ion-assisted deposition [47], deposition by RF plasma chemical reactor-supersonic plasma jet systems [124,125], shielded reactive vacuum arc deposition [126], molecular beam epitaxy (MBE) [33,45] or reactive pulsed laser deposition (RPLD) [44] – as it is of established RF and DC sputtering methods. Studies using these newer physical deposition methods are also focusing on how processing parameters can be managed to deposit copper nitride to prescribed standards.

2.2.2. Chemical deposition methods

Chemical deposition methods towards the fabrication of Cu_3N films mostly concern gas-phase processes, such as chemical vapor deposition (CVD) and atomic layer deposition (ALD). CVD and ALD processes were originally studied using precursors such as $Cu(hfac)_2$ and $[Cu(^sBu\text{-}Me\text{-}amd)]_2$ with an onus on determining the phase composition, growth rate and morphology of the resulting copper nitride films [127-131]. It should be noted, however, that none of these CVD or ALD syntheses involve single-source precursors and that combining the precursor with reactive ammonia gas in the reaction chamber is essential.

Just as ammonolysis reactions can be used to prepare bulk powder samples of copper nitride, as described in section 2.1.1, so it can also be applied for the fabrication of Cu_3N thin films, on the condition that substrate preparation (which might necessitate a prior precursor deposition step) is possible. The simplest form of such a reaction is arguably to ammoniate a copper surface directly and Terao originally performed such an ammonolysis experiment using metallic copper at 350 °C for 2 h [132]. The resulting films were characterised by electron diffraction. In recent years, two-step processes have been developed consisting of: (i) the deposition of a copper precursor followed by (ii) the ammonolysis of the fabricated layer. Szczęsny *et al.* reported preparation of microstructured Cu_3N thin films by the ammonolysis of a $Cu(CF_3COO)_2$ precursor using solution-based deposition techniques, such

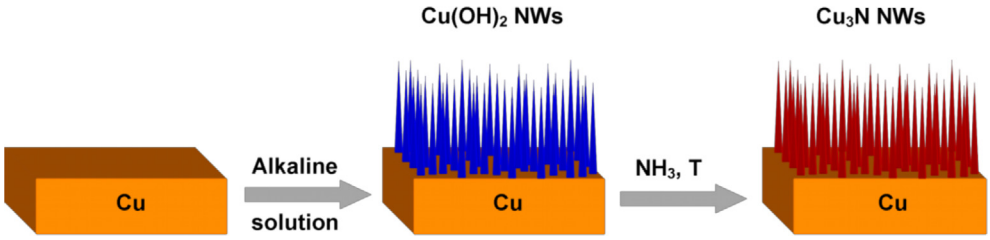

Fig. 5. A scheme for the synthesis of Cu_3N nanowires supported on copper foam.

as spin- and dip-coating or via nebulization [64]. The same authors attempted to utilize wet chemical deposition methods and copper (II) ketoxime complexes but homogeneous nitride films could not be realised [133].

Recently, the fabrication of copper nitride nanowire arrays grown on copper foam substrates has attracted considerable interest. The synthesis route starts from the growth of $Cu(OH)_2$ nanowires on a Cu foam in an alkaline solution of $(NH_3)_2S_2O_8$ and NaOH, followed by nitridation of the hydroxide nanowires under a flow of gaseous ammonia (Fig. 5) [134,135]. Similarly, Li *et. al.* synthesized a CoN/Cu_3N nanotube array decorated with carbon and supported on Cu foam using this facile method as a basis and investigated the applicability of the supported nanotubes to act as an electrocatalyst for overall water splitting [136]. The hierarchical nitride nanocomposite showed activity towards both the hydrogen and oxygen evolution reactions. Similar simple solution-initiated deposition methods can be used to fabricate many different arrays of related low-dimensional supported copper nitride nanostructures. These intricately designed structures have potential applications as supercapacitors or sensors [134,135,137]. One such example of a prospective device was constructed from Cu_3N nanowires grown on Cu foam combined with ultrathin CoFe-layered double hydroxide (LDH) nanosheets to form composite 3D hierarchical architectures termed as Cu_3N@CoFe-LDH core–shell nanowire arrays (NWAs) (Fig. 6) [137]. The asymmetric supercapacitors built from the high surface area Cu_3N@CoFe-LDH electrodes exhibit impressive energy densities of 2.474 mW h cm^3 and 92.6% reversibility after 10,000 cycles. The enhanced conductivity of Cu_3N cores in comparison with Cu-based oxides are a vital component towards achieving this level of performance. The latest research presents Cu_3N nanowire arrays synthesized also by an ammonolysis reaction but from copper(II) oxide precursors grown on electro- or PVD-deposited copper surfaces in an ammonia solution [138].

2.3. Properties and applications of binary copper nitride

Properties of copper nitride thin layers strictly depend on stoichiometry [139] and in many cases nonstoichiometric materials were deposited. In the case of bulk copper nitride these properties are more harmonised. Cu_3N is firmly established as a non-toxic, metastable intrinsic semiconductor characterised by a relatively high electrical resistivity and low reflectivity. The reflectivity of Cu_3N was studied in depth by Cremer and co-authors when they considered the applicability of the material for write-once optical data storage [31]. They determined that the laser induced decomposition of thin films resulted in a change in the reflectivity from 3.2% to 33.2% as nitrogen was removed from Cu_3N to form Cu metal. The optical energy gap (E_g) is one of the most important parameters that characterises semiconductors, especially in the context of materials design and the suitability of a semiconducting material for a given device and application. According to the literature, Cu_3N has an experimental band gap of between 0.8 and 1.9 eV [42,45,114,118,125]. Corresponding theoretical studies arrive at values that are generally smaller, ranging from 0.23 to ~ 1.0 eV [27,28,141,141], but it is not unusual for density functional theory (DFT) to underestimate the band gaps of solids. Here it is worth mentioning a recently published report on Cu_3N layers prepared from Cu on fused SiO_2, by heating under an NH_3:O_2 atmosphere. These layers exhibit maxima in the optical transmission related to the M and R direct energy band gaps of copper nitride, which are in very good agreement with density functional theory calculations (Fig. 7) [142]. In general, the size of the band gap depends on the experimental conditions, which in turn determine the chemical composition and microstructure of the material [143]. The possibility of the practical application of copper nitride is determined not only by the size of the band gap, but also by the stability of the material under ambient conditions and at elevated temperature. Compared to many more ionic nitrides, Cu_3N is quite stable under ambient conditions and can be stored over about 2 months, according to the literature [144]. Combination of both moisture and air at room temperature lead to the spontaneous degradation of Cu_3N to CuO. The exposure to deionized water for 15 days results in production of ammonia in 60% chemical yield (measured by the indophenol method) [66]. Copper nitride nanoparticles were also stable in buffer solutions, excluding ammonium acetate buffer, for 11 days [144]. The stability in air enables many typical operations and manipulations to be per-

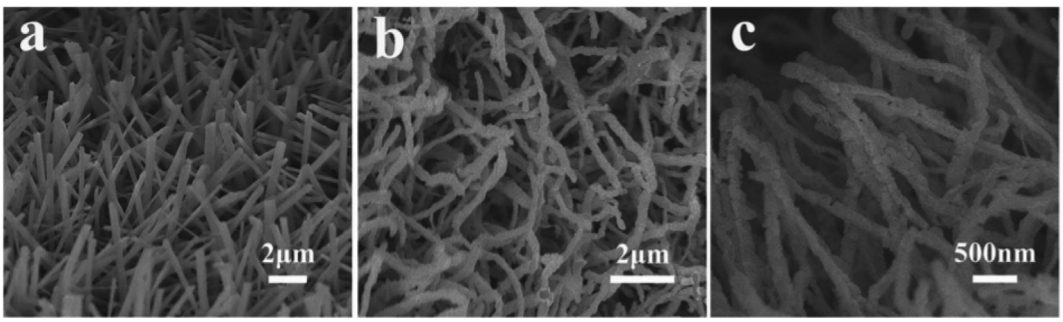

Fig. 6. SEM images of $Cu(OH)_2$ nanowire arrays (NWAs) (a) and Cu_3N NWAs (b, c). The figure was reproduced from Ref. [137] with permission from the rightsholders.

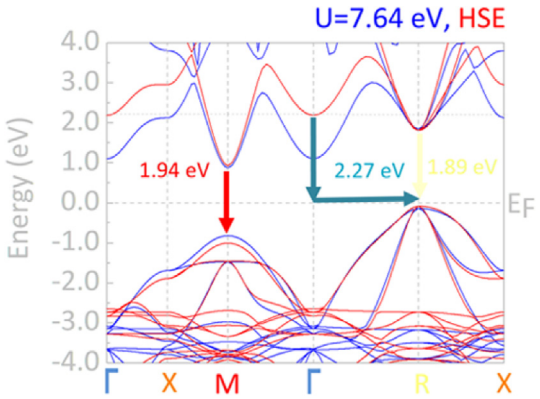

Fig. 7. Electronic band structure of Cu_3N with the M and R direct band gap transitions detected experimentally and with the Γ – R indirect transition. The figure was reproduced from Ref. [142] with permission from the rightsholders.

formed in ambient conditions and allows for generally unproblematic characterisation of Cu_3N. Given its acknowledged metastability, the thermal stability of Cu_3N is not high yet according to the literature, there is some discrepancy in its thermal decomposition temperature at ambient pressure; typically the decomposition of copper nitride films and powders can vary over a range of approximately 350 °C (from 100 °C to 450 °C), but the powders are reported to decompose from ca. 350 °C [35,50,64]. The lowest decomposition temperature detected for Cu_3N films annealed in vacuum conditions (pressure = $6{\cdot}10^{-4}$ Pa) amounted to 100 °C [39].

Applications of copper nitride have been mainly considered in the context of thin films until quite recently. Due to the low thermal decomposition temperature, low reflectivity and high electrical resistivity Cu_3N films were extensively studied towards their implementation in optical storage technology. Many authors have investigated the use of Cu_3N as a useful precursor to elemental copper and the transformation of copper nitride to metallic copper by thermal treatments [145,146], laser irradiation [36,47,148,148] or electron beam-induced decomposition [35,150,150]. The significant change in reflectance that occurs during this Cu_3N-Cu transformation signals the applicability of copper nitride as a material for use in optical data storage devices and the nitride is a very attractive non-toxic alternative to tellurium-based materials in this context [37,47,116]. The easily induced metallization process has been promoted to be a readily implementable way to generate microscopic Cu metal lines in the production of integrated circuits [147]. Furthermore, the electrical properties of Cu_3N itself are likely to be advantageous for spintronics applications and specifically to serve in low resistance magnetic tunnel junctions for magnetic random access memories [33,45]. Other novel applications where the development of copper nitride films can be seen as advantageous are based on the use of Cu_3N as a component in electronic devices such as thin-film transistors (TFTs) and complementary metal-oxide semiconductor (CMOS) circuits [151].

Aside from electronics, the major applications of copper nitride are likely to involve its integration into energy storage or conversion systems. Over the last 2 decades a growing number of investigations of copper nitride electrochemistry have lent support to its use as an electrode in lithium ion batteries [57,58,67,152]. Following original investigations by Pereira *et al.* where the behaviour of Cu_3N as a conversion anode was first mooted [55], subsequent studies have investigated the suitability of the material in both Li-ion and Na-ion cells. Li and co-workers, among others, used cyclic voltammetry to assess the performance of a Cu_3N electrode using powder prepared from a $Cu(OPiv)_2$ precursor in sodium and lithium half cells [67]. Stable cycling behavior was observed for Cu_3N both in sodium and lithium cells and for the latter an extremely impressive capacity of 1811 mA h g^{-1} was measured in the first cycle (at 0.5 C). The cycleability was not so impressive, however and by the 50th cycle the capacity dropped to 287 mA h g^{-1}. According to theoretical calculations, the large voids present in bulk Cu_3N crystals should be advantageous both in terms of high lithium mobility and the ability to store large amounts of lithium (thus achieving high specific capacity) [141]. Moreover, Cu_3N nanosheets were predicted to exhibit much lower energy barriers to lithium ion motion (ca. 0.09 eV) than other existing or proposed electrode materials, including graphene, for example (with an activation energy for Li-ion conductivity of 0.37 eV [153]). Furthermore, for hypothetical Cu_3N nanosheets the maximum capacity is predicted to reach 1008 mA h g^{-1} [141]. For comparison various transition metal compounds (oxides, sulfides, fluorides, nitrides etc.) can reach theoretical capacities of between 500 and 1500 mA h g^{-1} [154]. In contrast, commercial graphite electrodes exhibit a Li capacity of 372 mA h g^{-1} [155]. Given the prospects of high ionic and electronic conductivity when using Cu_3N as a conversion electrode, but noting also the less than spectacular reversible capacity, copper nitride would appear to be more viable as a component of the electrode–electrolyte interface than as an anode itself. With this in mind, copper nitride nanoparticles were combined with styrene butadiene rubber to form a layer not only with high ionic conductivity (when lithiated, Cu metal and fast ion conducting Li_3N are formed) but also with the high mechanical strength and flexibility that would subdue the dendrite growth that occurs on cycling a lithium metal anode. When tested as an artificial solid electrolyte interphase (SEI) layer the Cu_3N-rubber nanocomposite was found to sustain the performance and cycle life of a Li metal anode-lithium titanate (LTO) cathode cell considerably [156]. Recent work has built on this Cu_3N SEI principle either employing a copper nitride layer at the external surface of the copper current collector at the Li anode (in a cell using an $LiFePO_4$ cathode) or by printing Cu_3N nanowires directly on to the Li anode surface [157,158]. In this latter example, Cu_3N nanowires were transferred onto the surface of lithium foil by roll-pressing (Fig. 8). During operation this surface layer is converted

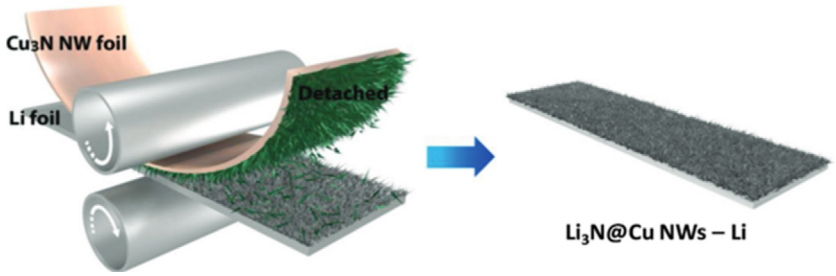

Fig. 8. The scheme of fabrication of Cu_3N NWs printed on Li foil by a roll-press method. The figure was reproduced from Ref. [158] with permission from the rightsholders.

to Li_3N/Cu nanowires. The Li_3N@Cu coating was used as an artificial SEI with an Li anode successfully over multiple cycles without significant capacity fade for cells with either an $LiCoO_2$ (300 cycles) or $Li_4Ti_5O_{12}$ cathode (1000 cycles) at a current density of 2 mA cm^{-2} [158]. Moreover, according to Park *et al.* [159], forming Cu_3N onto 3D Cu foam or 3D Cu rod surfaces allows for smooth Li stripping/-plating without dendritic growth of Li. The Li/3D Cu anodes prepared by this procedure exhibit stable long-cycle performance in symmetric cell tests.

Not only has copper nitride recently been shown to exhibit high electrochemical activity, but also it has been revealed to demonstrate appreciable catalytic activity for a range of important reactions. Cu_3N nanoparticles supported on superparamagnetic SiO_2 microspheres (Cu_3N/Fe_3N@SiO_2) were investigated towards the Huisgen 1,3-dipolar cycloaddition (HDC) of azides and alkynes (Scheme 2), which is a process conventionally catalysed homogenously using soluble Cu(I) complexes. All of the reactions performed in the presence of tertiary amines proceeded rapidly with good yields and high selectivity and with reaction kinetics comparable to the equivalent processes catalysed by the aforementioned Cu(I) complexes. Moreover, the Cu_3N catalyst is non-cytotoxic and easily recovered for further use, which makes it an extremely attractive alternative to the existing state of the art and encouraging for the development of a new generation of catalysts [63].

As briefly indicated above in the section on chemically-deposited thin films (section 2.2.2), substantial efforts have been made to investigate copper nitride as a new catalyst in the fields

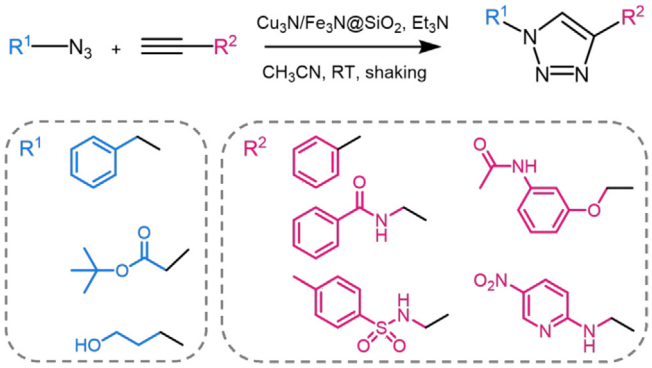

Scheme 2. The scheme for the synthesis of 1,2,3-triazoles using a Cu_3N/Fe_3N@SiO_2 catalyst. The figure was reproduced from Ref. [63] with permission from the rightsholders.

of sustainability, energy and the environment and not least in the context of water electrolysis. Exploration of the electroactivity of the nitride in the oxygen and hydrogen evolution reactions (OER, HER respectively) and also in the oxygen reduction reaction (ORR) has already shown that Cu_3N holds considerable promise for renewable energy production systems [55,78,79,87,93,159-162].

Encouragingly, recent reports also indicate that copper nitride can be used very effectively as a catalyst in the carbon dioxide reduction reaction (CO_2RR). Presently, Cu-based electro-catalysts are considered among the best suited for electrode materials in the CO_2RR, readily catalysing the reaction of CO_2 to hydrocarbons. However, studies now indicate that the selectivity offered by polycrystalline copper-based electrodes is not easily improved and a wide range of hydrocarbon products are often formed [163]. In an effort to overcome this problem, extensive research has been conducted on new Cu-based electrodes with the aim of reducing the required overpotential and of improving selectivity. Mi *et al.* synthesized Cu_3N-derived Cu nanowires which exhibited a maximum Faradaic efficiency of 86% at −1.0 V and stability over 28 h electrolysis [164]. The Cu_3N-derived nanowires offered superb C2 selectivity without a significant loss of activity and could constitute a future direction for electrocatalyst design for CO_2RR. Yin and co-workers went one step further and used nanostructures of Cu_3N itself as a highly effective CO_2RR catalyst [79]. They showed that Cu_3N nanocubes were stable and selective to ethylene production (yielding a C_2H_4:CH_4 molar ratio of greater than 2000) at −1.6 V, with a Faradaic efficiency of 60%. It was suggested that the high CO_2RR selectivity to C_2H_4 was dependent on the presence of Cu(I) and that the species was stabilised within the Cu_3N structure. Liang *et al.* indicated that Cu_3N fulfilled a role as an inert support modifying the electronic structure of Cu metal at the surface (Fig. 9) [165]. This catalyst showed higher selectivity towards C_{2+} species formation than was observed when using either CuO or pure Cu as an alternative. It is already evident from these recent studies that not only is Cu-Cu_3N a very promising catalyst combination for CO_2 reduction but also that with further understanding of the role of each component, it should be possible to tune the stability, activity and selectivity further [166].

3. Multinary copper-based nitrides

We would like to start by defining the scope and limits of this section. The physical and chemical approaches to the deposition of copper nitride thin films were covered in detail in the sections above. As briefly alluded to in those sections, the doping of films

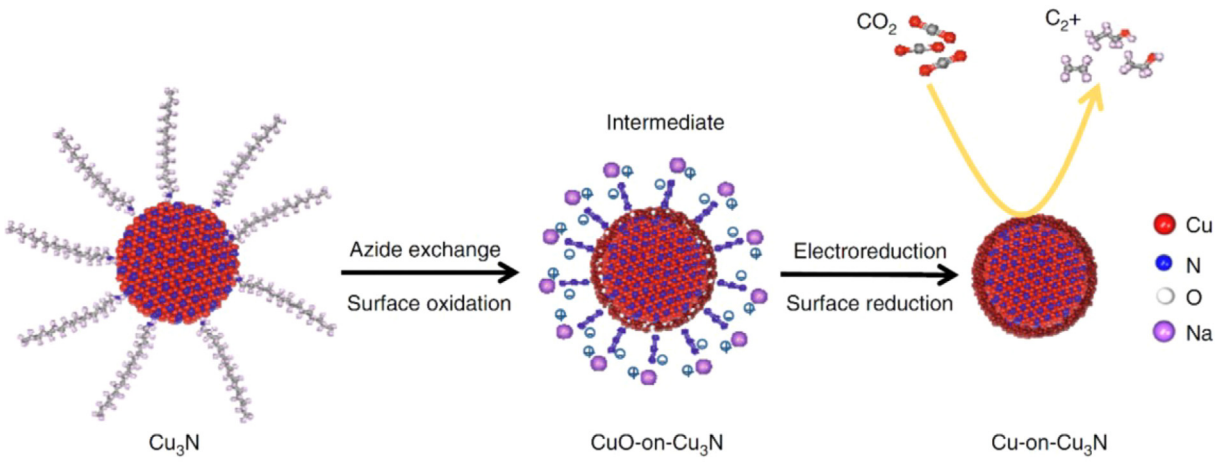

Fig. 9. Synthesis scheme for a Cu-on-Cu_3N catalyst. The figure was reproduced from Ref. [165] with permission from the rightsholders.

to increase compositional complexity and to induce new behaviours is an important part of nitride thin film research. Such doping of PVD- and CVD-deposited Cu_3N films to create pseudo-ternary and higher compositions has been discussed comprehensively in a recent review and we do not intend to repeat that information here [53]. Rather, in this section we would like to focus on compounds representing families of complex (multinary) copper nitrides, which can be synthesised as bulk powders, nanoparticles or single crystals by chemical rather than physical methods. These compounds are intrinsically very difficult to prepare and handle and consequently it is unsurprising that only a handful of these have been described to date.

3.1. Preparation and structural characterisation

Extensive studies have provided an array of synthetic methods that give access to a wide range of compounds spanning very different structures in which Cu–N bonding is present. These examples encompass well-known structure types such as (*anti*-) perovskite and delafossite, as well as compounds that exhibit unprecedented crystal structures that typically contain infinite -Cu–N- chains, discrete copper nitride units, or a mix thereof. The predominant oxidation state of copper is + 1 throughout and it is worth mentioning that in all reported compounds, the Cu(I) ions are linearly coordinated by N atoms with bond lengths remaining close to a value of 1.9 Å. In fact, the longest Cu–N distances in an inorganic nitride were revealed in a set of compounds containing Ta or Nb (with Cu–N distances of 2.08 Å and 2.07 Å respectively) [167-169]. This moderate increase in bonding distance has been explained by the fact that corresponding Ta/Nb-N interactions are significantly covalent in character and stronger than those observed with, for example, alkaline earth metals in ternary and higher nitrides [170].

3.1.1. Ternary copper nitrides

3.1.1.1. Compounds with the anti-perovskite structure, Cu_3M_xN. It is perhaps not surprising that copper is able to form *anti*-perovskite nitrides given that the structure of the binary compound, Cu_3N, is already so closely related. The *anti*-ReO_3 copper(I) nitride structure transforms to that of perovskite simply by the occupation of the cubic body centre (Fig. 10).

The first of the *anti*-perovskite copper nitrides were discovered in 1991. The two compounds Cu_3Pd_xN, with M = Pd occupying the central voids present in the Cu_3N framework (Fig. 10), were reported with x = 0.020(3) and 0.989(5) [25]. The cubic unit cell expands as a result of progressive Pd insertion with a = 3.812(1) Å and a = 3.850(1) Å for x = 0.020(3) and x = 0.989(5) respectively. (In fact, the cell volume of the ternary nitrides appears to initially contract on the introduction of Pd as compared to the parent, Cu_3N; a = 3.817(1) Å). The compounds were prepared at high pressure and high temperature by reacting $[Cu(NH_3)_2]NO_3$ with $[Pd(NH_3)_4](NO_3)_2$ in supercritical ammonia at 500 °C and $P(NH_3) \approx 6$ kbar in autoclaves. The silver-coloured phases appeared to be metastable by analogy to the parent Cu_3N and decomposed at 470 °C (a comparable temperature to Cu_3N under similar conditions [70]) to Cu_3Pd_x and N_2. The fact that the reaction conditions were not extremely harsh and that the decomposition temperature is not overly high meant that Cu_3Pd_xN *anti*-perovskites were excellent candidates to target via alternative and gentler synthesis methods. It was considered that nanoparticles might exist as more stable alternatives to the metastable microcrystalline bulk powders. It thus transpired that Cu_3PdN was the first ternary metal nitride prepared in the form of colloidal nanocrystals, which were obtained by heating copper(II) nitrate and palladium(II) acetylacetonate in 1-octadecene with oleylamine under inert atmosphere to 240 °C and keeping the reaction at this temperature for 10 min [59].

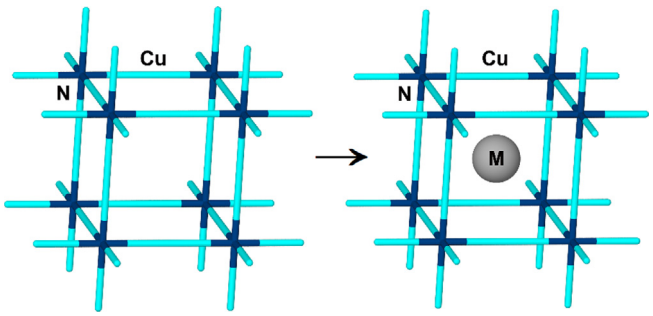

Fig. 10. Schematic showing the relationship between the *anti*-ReO_3 structure of Cu_3N (left) and the *anti*-perovskite structure of the ternary nitrides, Cu_3M_xN (right).

A second series of *anti*-perovskites was reported in 2004 as a result of attempts to insert Li cations into the Cu_3N framework [26]. To achieve this, the authors attempted a typical chemical lithiation procedure in which freshly prepared Cu_3N was reacted with n-butyllithium at 60 °C. The reactions resulted in black powders of composition Li_xCu_3N ($0 \leq x \leq 1$). The anticipated intercalation was not straightforward and was accompanied by a substitution of Cu^+ by Li^+ in parallel. The reaction products could be formulated as $Li(2)_{x-y}Cu(2)_y[Li(1)_yCu(1)_{3-y}N]$, where (citing the authors) "x stands for the amount of intercalated Li determined by chemical analyses and y for the amount of Cu being replaced by Li, as determined by structure refinement". This implies that in the case when x = y, an *anti*-perovskite structure exists with (reduced) metallic copper captured inside the body centered voids of the parent framework. It is also worth mentioning here that the successful synthesis of ternary lithium copper nitrides had already been achieved more than 50 years earlier, in 1949 [171]. However, the original syntheses involved the reaction of lithium nitride with metallic copper under a nitrogen atmosphere at 700 °C (with the reaction initiating at ca. 620 °C). This was thus the "inverse" of the chemical lithiation reaction (Cu(I) + Li(0) vs. Li(I) + Cu(0)) and the reaction products were entirely different, being the solid solution of ternary compounds, $Li_{3-x}Cu_xN$ ($0 \leq x \leq 0.3$) [172]. Interestingly, however, both these reactions are effectively topotactic, with the M(0) reactant integrated into the parent structures of the respective binary nitrides (either Cu_3N or Li_3N).

3.1.1.2. Compounds with the delafossite structure. The novel and isostructural ternary copper nitrides of formula $CuMN_2$ (M = Nb, [167] Ta [168,169]) were obtained in solid state ion exchange reactions, in which the pre-synthesised ternary nitride precursor $NaMN_2$ was combined with a 5-fold excess of CuI under a nitrogen atmosphere. In the case of Nb, this process could be achieved at 300 °C, whereas the equivalent Ta reaction required a higher temperature of 400 °C; both reactions were complete over 48 h. The two ternary $CuMN_2$ compounds form with the delafossite structure (Fig. 11) which, despite the presence of linear N-Cu–N units, is otherwise very different from the *anti*-ReO_3 structure of Cu_3N. In fact, the $CuMN_2$ nitride structures are more closely related to the $NaMN_2$ reaction precursor (with the α-$NaFeO_2$ structure); both structures contain MN_2 layers and differ principally in the positions of the Na(Cu) atoms between the planes. As a result, despite both starting material and products having the same space group, $\bar{R}3m$, the Na or Cu atoms between MN_2 layers are octahedrally or linearly coordinated by nitrogen respectively.

3.1.1.3. Compounds with structures containing bent -Cu–N- nitridocuprate chains. There are two known ternary compounds of this

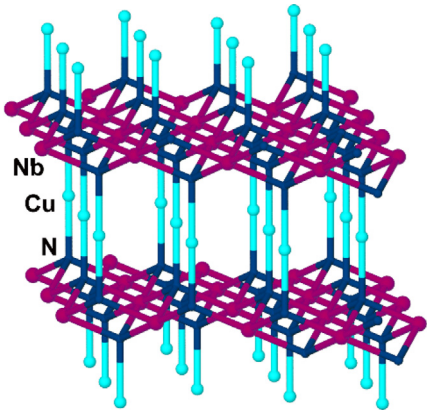

Fig. 11. Representation of the delafossite structure of $CuNb(Ta)N_2$ with $Nb(Ta)N_6$ octahedra arranged in layers which are interconnected by linear N–Cu–N units.

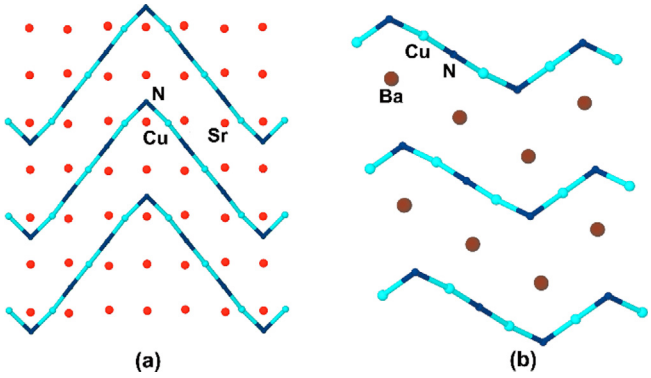

Fig. 12. Representations of the infinite nitridocuprate 1D zig-zag chains present in (a) SrCuN and (b) BaCuN.

type, which have the general formula ACuN (A = Sr [173], Ba [170]). Both can be synthesized in adapted solid state reactions with the addition of a Na flux (liquid Na) to the solid state starting materials. The method takes advantage of the low melting point (98 °C) of metallic Na, and has proved increasingly popular in the synthesis of ternary and higher nitrides since it facilitates the dissolution of nitrogen-containing polyatomic species while depressing the crystal growth temperature below the decomposition temperature of the product(s) [174]. This technique appears to function best for nitrides with some degree of ionic character, particularly those containing alkali and alkaline earth metals, which have superior solubility in sodium. Moreover, the sodium flux method can be applied to the synthesis of a range of nitrides of which the ACuN compounds are just a small subsection (although it appears most suited to nitride structures containing discrete or 1D chain complex anions, which could be a reflection of the solubility limits of nitrogen in the sodium melt).

The synthesis of SrCuN (black crystals) was performed in an autoclave using Cu_3N powder, strontium pieces and NaN_3 as a source of both sodium and nitrogen. The reaction involved heating at a rate of 100 °C h^{-1} to 800 °C and soaking for 24 h before cooling to 500 °C over a period of 99 h. Above 300 °C, the sodium azide decomposes rapidly to sodium and nitrogen, producing a maximum nitrogen pressure of ca. 25 bar at 800 °C [173]. The authors also report that SrCuN can be accessed via an alternative reaction under less extreme conditions in which Sr_2N and Cu_3N powder (1:1) are heated under 1 bar of nitrogen pressure at 800 °C for 48 h [175]. The structure of the product, crystallising in the orthorhombic *Pnma* space group (a = 9.045(2) Å, b = 13.234(3) Å, c = 5.388(1) Å), shows the presence of infinite, zig-zag 1D -Cu–N- chains, which are kinked at every fourth N atom (or after every third N-Cu–N dumbbell) (Fig. 12a). One remarkable feature of the structure is the short intrachain distance between the closest Cu-Cu ions in the zig-zag chains (between Cu atoms across a chain kink, 2.476(3) Å), indicating the presence of rather significant cuprophilic interactions (by comparison, the single Cu-Cu bond in the diatomic Cu_2 molecule is 2.22 Å while in the solid state, the Cu-Cu distance in metallic copper is 2.56 Å) [176]. The zig-zag chains run along the *b*-axis of the unit cell, with their packing adopting a herringbone motif.

The synthesis of closely related BaCuN (black crystals) differs from that of SrCuN mostly in the use of Cu_2O or Cu rather than Cu_3N as the copper-containing starting material. Thus, Cu_2O(1)eq uivalent/Cu(1)equivalent, $BaN_{0.78}$(4)equivalents/Ba(2)equivalents, NaN_3 and sodium were sealed under argon in a niobium tube and heated to 800 °C over a period of 12 h. After a further 12 h at this reaction temperature, the tube was slow-cooled to ambient temperature over 100 h [170]. The sodium flux needs to be removed post-reaction in order to isolate the crystalline ternary nitride product and this is effectively achieved by washing or extracting with dry liquid ammonia.

Interestingly, BaCuN is not isostructural with SrCuN (*C*2/*c* space group of a monoclinic system with *a* = 14.462(2) Å, *b* = 5.5700(8) Å, *c* = 9.478(1) Å, β = 102.960(2)°). The zig-zag chains formed in this case are asymmetric about each kink, each of which forms at every third and second nitrogen, alternately (or after every 2 and 1 N-Cu–N dumbbells) (Fig. 12b). The closest intrachain Cu-Cu distance, which is between Cu atoms across a chain kink, is equal to 2.490 (2) Å, which is virtually the same as that in the corresponding strontium compound, again indicating the presence of notable cuprophilic interactions.

3.1.1.4. Compounds with structures containing mixed complex nitridocuprate anions. There are a few examples of ternary copper nitrides containing both the linear and bent moieties that exist otherwise individually as described in the examples in the previous sections above. In fact, the kinked chains in SrCuN and BaCuN could be considered as V-shaped units and linear dumbbells connected by vertices to propagate infinitely in one crystallographic direction. In contrast, metallic blue $Sr_6Cu_3N_5$ forms a structure containing linear $(CuN_2)^{5-}$ and V-shaped $(Cu_2N_3)^{7-}$ nitridometallate anions as separate isolated species [173]. Interestingly, this compound was obtained as one of the co-products in the above-mentioned sodium flux synthesis of SrCuN, using high pressure nitrogen in an autoclave. The highest yield of $Sr_6Cu_3N_5$ was achieved using a Sr:Cu:NaN_3 ratio of 1:2:10. The Cu(I) species present in each complex anion can be clearly regarded as chemically-different rather than simply crystallographically inequivalent. As seen in the chain kinks of SrCuN and BaCuN, there is a significant interaction between copper ions across the width of the V-shaped anions. The Cu---Cu distance of 2.448(4) Å is very similar

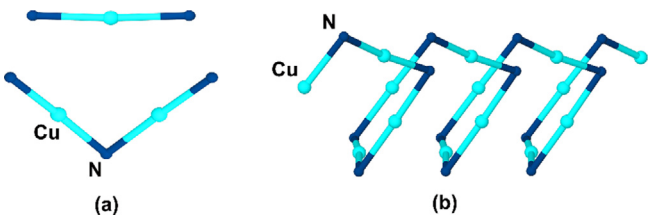

Fig. 13. Representations of the complex nitridocuprate anions present in $Sr_6Cu_3N_5$ and $Ba_{16}[(CuN)_8][Cu_2N_3][Cu_3N_4]$; (a) linear $(CuN_2)^{5-}$ and V-shaped $(Cu_2N_3)^{7-}$ units in $Sr_6Cu_3N_5$; (b) fragment of a helical chain in $Ba_{16}[(CuN)_8][Cu_2N_3][Cu_3N_4]$.

– although notably even shorter – than that in the infinite chains of the 1:1:1 compounds (Fig. 13).

The black barium nitridocuprate, $Ba_{16}Cu_{13}N_{15}$, which is more helpfully formulated as $Ba_{16}[(CuN)_8][Cu_2N_3][Cu_3N_4]$, was obtained by following the same synthesis procedure as that for BaCuN, but by using a 1:5 M ratio of Cu:Ba and with barium nitride formed as by-product [170]. The nitride has a crystal structure comprised of an even more complex variety of nitrodocuprate anion geometries. Each of these anions can again be viewed as being constructed from discrete linear $[Cu_2N_3]^{7-}$ dumbbells and Z-shaped $[Cu_3N_4]^{9-}$ units. Meanwhile, the remaining infinite -Cu–N- helical chains can be construed as a continuous ribbon of vertex-connected V-shaped units (Fig. 13b). Since the compound crystallises in the centrosymmetric monoclinic $P2_1/c$ space group, the CuN chains present in the structure rotate in both senses relative to the propagation direction. The closest contact between Cu-Cu ions in the helical chains is 2.668(5) Å, which is strikingly longer than the equivalent distances seen in the kinked chains of BaCuN. The helical chains form pseudo-layers which are separated by layers of discrete anions.

3.1.2. Quaternary copper nitrides

3.1.2.1. Compounds with structures containing either discrete or infinite chain nitridocuprate ions. There are relatively few known quaternary nitridocuprates and $Ca_4Ba[CuN_2]_2$ is the only one of these to contain only discrete complex anions (of any type). The nitride was obtained as black crystals from a mixture of Cu, Ca and Ba (2:1:1) following a synthetic procedure otherwise very similar to that for the preparation of BaCuN. Large amounts of unreacted copper and barium nitride were found in the reaction product [170]. The crystal structure (tetragonal, $P4/ncc$ space group, a = 8.2366(4) Å, b = 12.5731(6) Å) is perhaps surprisingly simple in view of the structures of similar alkaline earth metal-containing ternary compounds and the additional compositional complexity of $Ca_4Ba[CuN_2]_2$. Nitridocuprate ions are present only as discrete linear $[CuN_2]^{5-}$ dumbbells, which form pseudo-layers together with the alkaline earth ions.

Two isolated compositions in the Sr–Ba–Cu–N quaternary system were obtained as non-stoichiometric compounds, namely, $Sr_{0.53}Ba_{0.47}CuN$ and $Sr_{0.9}Ba_{0.1}CuN$. Each was prepared under similar conditions to $Sr_8Cu_3In_4N_5$, as described in the next section, using Sr:Ba molar ratios of 1:1 or 1.5:1, respectively [177]. Interestingly, structural studies revealed the presence of different types of nitridocuprate infinite zig-zag chains in each of the crystal structures. A symmetrical zig-zag chain with four connecting N-Cu–N "links" in each repeat unit of the chain (i.e. with a kink at every third nitrogen; after every second N-Cu–N dumbbell) was revealed in the former, with a closest Cu---Cu distance of 2.4728(13) Å. This might also be viewed as an infinite chain of vertex-sharing, alternately-inverted V-shaped (N–Cu–N–Cu–N) units, thus resembling a saw-tooth wave (Fig. 14). By contrast, the chain motif in $Sr_{0.9}Ba_{0.1}CuN$ is almost identical to that in the compositionally very similar SrCuN; namely with six N-Cu–N links in each repeat unit of the chain (i.e. with a kink at every fourth nitrogen), with a much shorter closest Cu---Cu distance of 2.36 Å). By comparing the structures of these two quaternary compounds, $Sr_{0.53}Ba_{0.47}CuN$ and $Sr_{0.9}Ba_{0.1}CuN$ and also the "parents" BaCuN and SrCuN, it is apparent that the number of N-Cu–N links in each repeat unit of the chain is dependent on the (average) size of the respective alkaline earth cation, with an increasing cationic radius correlating with zig-zag chains with fewer links per repeat unit (and thus a higher concentration of kinks).

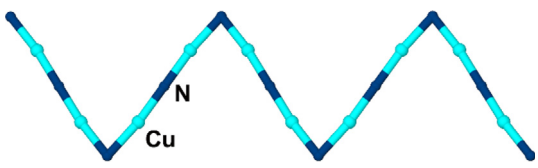

Fig. 14. Fragment of the type of infinite nitridocuprate 1D zig-zag chain present in $Sr_{0.53}Ba_{0.47}CuN$.

3.1.2.2. Compounds with structures containing both discrete and infinite nitridocuprate ions. A series of intriguing indium-containing quaternary nitridocuprates were each also synthesized by sodium flux methods. Each of these compounds are noteworthy not only because of the diversity of the component copper anions but also due to the co-existence of In Zintl clusters within the same structures. The isostructural black metallic nitrides, $Ba_8Cu_3In_4N_5$ [178] and $Sr_8Cu_3In_4N_5$ [177] were prepared via an Na flux method in which Ba (or Sr), Cu, In and Na were mixed in a molar ratio of 2:1:1:6 and heated following a complex temperature regime under 7 MPa pressure of N_2. Initially the reactants were heated to 1023 K for 1 h, before slow cooling first to 823 K at a rate of 2 K h^{-1} followed by natural cooling to room temperature. High purity single crystalline products were obtained by washing in liquid NH_3 to remove remnants of the Na flux. The structures show the presence of very different structural units. Complex nitridocuprate anions are present as both infinite chains and discrete units whereas the indium exists entirely in the form of homoatomic Zintl polyanions, which themselves self-organise into infinite chains of metal clusters (formed from the edge sharing of two crystallographically-in equivalent In_4 tetrahedra) (Fig. 15).

A third compound of this general type, $Ba_{14}Cu_2In_4N_7$, was also obtained by a sodium flux method similar to that described for $Ba_8Cu_3In_4N_5$ above, in this case using a larger amount of Ba starting material (a Ba:Cu:In:Na molar ratio of 6:1:1:6 was employed) [179]. This compound can be classified as a subnitride (with tentative charge allocations of $(Ba^0)(Ba^{2+})_{27}(N^{3-})_6([CuN_2]^{5-})_4([In_4]^{8-})_2$ and contains isolated $[CuN_2]^{5-}$ nitridocuprate units and no equivalent infinite chains, however. The indium exists in isolated $[In_4]^{8-}$ clusters. With a recent resurgence of interest in Zintl cluster chemistry, [180] these unusual hybrids have attracted curiosity in terms of their fundamental inorganic chemistry, but could also prove to have intriguing properties. Thus far, preliminary tests have shown them to be metallic.

3.2. Properties and applications

Structural studies are often the first step towards uncovering new applications. With regards to ternary and complex nitrides and as shown in a recent review, [181] structure–property relationships are relatively well understood for the *anti*-perovskite nitrides and with respect to copper, it is this family of multinary nitrides that are consequently perhaps closest to potential applications. The ternary *anti*-perovskite nitrides, Cu_3Pd_xN can be switched from semiconductors to semimetals by increasing the amount of Pd inserted into the *anti*-ReO_3-type structure of Cu_3N. Computational studies reveal that a transition from essentially covalent bonding to metallic bonding as Pd is introduced is mainly caused by the hybridisation of Pd 5 s and 5p states with Cu 3d states [28]. It was also suggested (based on computational studies) that Cu_3PdN could exist as new three-dimensional Dirac semimetals showing unique transport properties, [182,183] but this hypothesis was not confirmed by studies performed on thin films of the compound [184]. The successful synthesis of colloidal nanocrystals of Cu_3PdN has also had a big impact in terms of new properties and applications. Nanoparticles of the ternary nitride have proven to be promising and highly active electrocatalysts for the oxygen reduction reaction (ORR) under alkaline conditions, proving to demonstrate competitive or higher ORR activity to

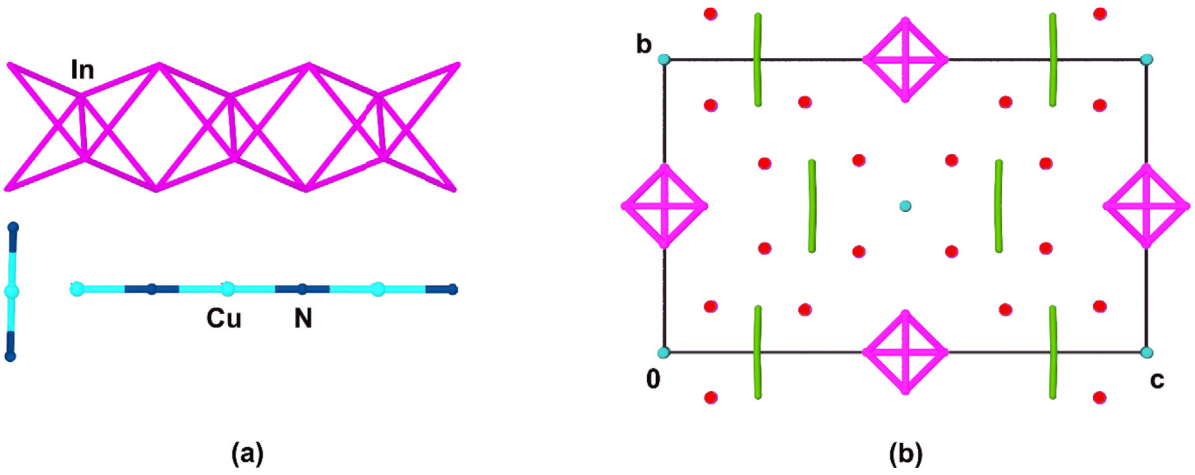

Fig. 15. Representation of (a) the species present in isostructural Sr/$Ba_8Cu_3In_4N_5$ compounds; alkali earth metals omitted for clarity, (b) packing shown down the a axis, discrete N-Cu–N units presented in green, 1D linear –Cu–N– chains in blue, Ba/Sr cations in red.

similarly synthesised nanoparticles of Pd and Cu_3N respectively. Moreover, nanoparticles of Cu_3PdN exhibit higher cycling stability than Pd equivalents [59].

Equally, however, novel applications are also emerging for ternary compounds with delafossite type structures. The delafossites appear to have good prospects as energy conversion materials particularly as absorbers in solar energy conversion, [185] but also, potentially as thermoelectrics for the harvesting of waste heat [186]. In the latter context, calculations indicate that $CuTa(Nb)N_2$ might emerge as promising p-type thermoelectrics, but their properties and performance are difficult to predict with precision given that their electronic structures vary depending on the calculation method employed (Generalized Gradient Approximation Perdew–Burke–Ernzerhof functional potential; GGA-PBE vs. modified Becke–Johnson; mBJ methods). Figures of merit, zT, of ca. 0.5 were predicted but, ultimately, practical application is likely to be limited by their low decomposition temperatures.

Conversely, the delafossite copper nitrides possess impressive optical properties that should favour solar conversion applications, particularly when compared to binary Cu_3N, for example. Particularly problematic for the latter in this regard is that the optical absorption onset occurs 0.4 eV higher than the 1.0 eV indirect fundamental band gap, which is not optimal for photovoltaics. The value of 1.5 eV determined experimentally for $CuTaN_2$ is close to optimal and correlates well with DFT calculations, which suggest a direct band gap of 1.4 eV [169]. Subsequent investigations showed that the analogous niobium delafossite, $CuNbN_2$ possesses a direct band gap of 1.3 eV (with an indirect gap of 0.9 eV) which has sparked considerable interest in these materials. Their prospects are enhanced further by their stability; although both $CuTaN_2$ and $CuNbN_2$ are thermodynamically metastable, they exhibit kinetic stability over lifetimes of many years. In fact, it is worth noting that the thermodynamic instability of the delafossite copper nitrides arises primarily due to the high binding energy of N_2 as compared to the Cu–N bond formation energy, but that in terms of enthalpy, decomposition to Nb_5N_6, Cu and N_2 is computationally predicted as favoured over decomposition to the elements. This outcome becomes even more favourable when considering the entropy contribution of N_2 gas [167].

As illustrated by the preparation of multinary nitridocuprates via the Na flux method in the previous section, synthesis routes to complex compounds – and especially nitrides – can often lead to unanticipated products, which in many cases co-exist with other phases and can only be retrieved as single crystals. Such reactions can be difficult to control and can involve various degrees of serendipity. However, these fundamental studies can, in many cases, lead to more targeted syntheses subsequently and opportunities to apply rational design as understanding of the compositional systems increases. Nevertheless, the preparation of higher metal nitrides is not a trivial task and an alternative approach that is gaining increased traction is to undertake computational studies *prior to synthesis* to identify hypothetical compounds with specific properties that could in all likelihood exist thermodynamically. This so-called inverse design strategy is a novel approach in materials science, with functionality being the first step in the design process (i.e. in the preparation of a compound with the predicted desired properties) [187,188]. This philosophy was adopted recently to construct a first comprehensive stability map of ternary nitrides; seven new nitrides were subsequently realised experimentally as thin films by sputtering. [189]. While identifying new thermodynamically-stable ground-state materials is ultimately the desired result of such predicative forays, it is notable among nitrides – and copper nitrides are a particularly good example - that metastable phases constitute many of the compounds discovered to date and that those with good kinetic stability (such as the delafossites above), can also be prime candidates for a range of practical and viable applications. With solar energy conversion the priority, a more focused computational study was performed to predict ternary Cu-M–N materials and their crystal structures [167]. The DFT calculations accomplished by Zakutayev *et al.* predicted the thermodynamic stability of 44 copper nitrides with stoichiometries, $Cu_xM_yN_z$ (where $z < 4$ and x, y, z are integers) which fulfil the octet rule. An analysis of the optical properties of these solids was conducted on the provision that greater than 30% efficiency should be achievable for semiconductors with absorption at band gaps, E_g of 0.8–1.7 eV [190]. The search led to seven compounds deemed worthy of further study; SrCuN, $CuNbN_2$, $CuTaN_2$, MgCuN, CaCuN, $Cu_3Ga_2N_3$, and Cu_3In_2N. Of these, the first three compounds were already known (see above), with the properties of $CuNbN_2$ and $CuTaN_2$ already known to be favourable. The remaining four compounds are still to be experimentally realized and it will be extremely interesting to see if they are discovered in the coming years.

4. Conclusions

The chemistry of transition metal nitrides continues to reveal both opportunities and challenges throughout the materials development cycle, from synthesis through to practical applications. In

this review we have sampled a small section of this growing field by presenting the current state-of-the-art in the chemistry of binary and higher copper based nitrides as obtained as bulk powders and crystals or in thin film form. We have explored the wealth of now available synthetic pathways to both the parent binary nitride and to substituted/doped variants and examined how the choice of preparation route affects the final products; in the case of thin film fabrication, preparation can be via physical deposition methods as well via chemical processes. The formation of copper nitride thin films is pivotal on modes of developing Cu–N bonds by inserting adsorbed N atoms into a lattice of Cu atoms. There are many sophisticated ways in which this can be achieved and the constant improvements made in film homogeneity and quality have spurred on research concerning the electrical and optical properties of both stoichiometric and non-stoichiometric Cu–N thin films. Moreover, reproducible methods of doping such films lend additional versatility to the devices that can be created, expanding the range of potential applications. Physical properties of copper nitride thin films can be manipulated by judicious doping of main group metals (Li, Al, Pb), other transition metals (e.g. Ti, Ni, Zn, Cr, Fe, Mn, Sc, Pd etc.), lanthanides and even non-metals. In many cases, the fundamental chemistry and physics that underpins the formation and function of these materials (such as doping mechanisms, the solubility limits of the doping atoms and their location in the Cu_3N structure and the effects of optical impurities) remain to be elucidated.

Bulk copper nitride powders (crystallites) have been prepared almost exclusively by chemical synthesis techniques, and the solid state chemistry is dominated by the only well-characterised compound in the binary system, Cu_3N (a likely line phase). Despite the evident stoichiometric rigidity of the binary nitride and the lack of apparent polymorphs, it is possible to prepare many different morphological forms of copper nitride at the micron scale and below; the growth and resulting size and shape of such particles can be very sensitive to physical and chemical synthesis with significant implications for the physical properties of the synthesized materials. The control of electronic and optical properties is particularly important for the potential applications of this narrow band gap semiconductor, but equally surface reactivity is proving decisive in new developments of the material as a catalyst to rival less naturally abundant and more expensive already-established competitors. Moreover, whereas the chemistry and physics of Cu_3N are now relatively well-studied, the same cannot be said for those of the ternary and higher copper nitrides. In fact, still only a handful of multinary copper nitrides are known and studies are largely limited to their synthesis and crystal chemistry. Their local structures are dominated by the same linear N-Cu–N units observed in Cu_3N, yet their extended structures can be entirely different and 1D and 2D structures prevail, whether these are based on known oxides (e.g. delafossite) or adopt unprecedented structure types. It is also apparent that the just as much of the chemistry of oxide cuprates is governed by Cu(II), flexible coordination geometries and the Jahn-Teller effect, so both binary and higher copper nitrides focus on Cu (I) in low coordination environments. It remains to be seen whether these valence and bonding restrictions are universal and what effect this has on physical properties as more complex nitrides are discovered.

Cu_3N and certain ternary nitride semiconductors (e.g. the delafossites, $CuTa(Nb)N_2$) already show promise for development in optoelectronic devices, catalytic systems, as composite electrodes in batteries and supercapacitors or for solar energy conversion. It seems likely that further useful properties and applications will be discovered for Cu_3N and for ternary nitrides with known structural analogues in, for example, oxide chemistry. For other ternary and higher copper nitrides, the systematic measurement of physical properties is yet to begin but as this uncharted territory is explored, one might hope and expect the unearthing of new functional materials. It is nonetheless clear, however, that much of the basic inorganic, solid state and materials chemistry research is currently missing and that this fundamental research is essential to expand the range of known copper (and other transition metal) nitrides. Until the location of the boundaries of nitride existence becomes clearer, it will not be possible to develop the level of understanding in structure and bonding that allows the materials design process to take place. Besides the materials discovery process that is achieved via novel synthesis, advanced computational approaches will be vital in predicting where the synthetic chemist might look. Indeed, the interaction between experimental and theoretical scientists will be vital for the progression of copper nitrides just as it is in so many other spheres of modern science.

Declaration of Competing Interest

The authors declare that they have no known competing financial interests or personal relationships that could have appeared to influence the work reported in this paper.

Acknowledgement

A.Ś., E.S., L.D. and R.S. acknowledge the "Excellence Initiative – Research University" NCU programme (pl IDUB).

DHG acknowledges the EPSRC, UK (grants *EP/N001982/1; EP/I022570/1*) and the University of Glasgow for funding associated with this work.

References

[1] N. Tapia-Ruiz, M. Segalés, D.H. Gregory, The chemistry of ternary and higher lithium nitrides, Coord. Chem. Rev. 257 (13-14) (2013) 1978–2014, https://doi.org/10.1016/j.ccr.2012.11.008.

[2] S.T. Oyama, The Chemistry of Transition Metal Carbides and Nitrides, Springer, Netherlands, Dordrecht (1996), https://doi.org/10.1007/978-94-009-1565-7.

[3] D.H. Gregory, Structural families in nitride chemistry, J. Chem. Soc. - Dalt. Trans. (1999) 259–270, https://doi.org/10.1039/a807732k.

[4] D.H. Gregory, Nitride chemistry of the s-block elements, Coord. Chem. Rev. 215 (1) (2001) 301–345, https://doi.org/10.1016/S0010-8545(01)00320-4.

[5] M.A. Brogan, R.W. Hughes, R.I. Smith, D.H. Gregory, Structural and compositional tuning of layered subnitrides; new complex nitride halides, Dalt. Trans. 39 (2010) 7153–7158, https://doi.org/10.1039/c0dt00214c.

[6] D.H. Gregory, P.M. O'Meara, A.G. Gordon, D.J. Siddons, A.J. Blake, M.G. Barker, T.A. Hamor, P.P. Edwards, Layered ternary transition metal nitrides; synthesis, structure and physical properties, J. Alloys Compd. 317–318 (2001) 237–244, https://doi.org/10.1016/S0925-8388(00)01340-2.

[7] D.H. Gregory, P.M. O'Meara, A.G. Gordon, J.P. Hodges, S. Short, J.D. Jorgensen, Structure of Lithium Nitride and Transition-Metal-Doped Derivatives, $Li_{3-x-y}M_xN$ (M = Ni, Cu): A Powder Neutron Diffraction Study, Chem. Mater. 14 (2002) 2063–2070, https://doi.org/10.1021/cm010718t.

[8] R. Niewa, F.J. DiSalvo, Recent Developments in Nitride Chemistry, Chem. Mater. 10 (10) (1998) 2733–2752, https://doi.org/10.1021/cm980137c.

[9] R. Niewa, H. Jacobs, Group V and VI Alkali Nitridometalates: A Growing Class of Compounds with Structures Related to Silicate Chemistry, Chem. Rev. 96 (1996) 2053–2062, https://doi.org/10.1021/cr9405157.

[10] F.J. DiSalvo, S.J. Clarke, Ternary nitrides: a rapidly growing class of new materials, Curr. Opin. Solid State Mater. Sci. 1 (2) (1996) 241–249, https://doi.org/10.1016/S1359-0286(96)80091-X.

[11] A. Kilicaslan, O. Zabeida, E. Bousser, T. Schmitt, J.E. Klemberg-Sapieha, L. Martinu, Hard titanium nitride coating deposition inside narrow tubes using pulsed DC PECVD processes, Surf. Coat. Technol. 377 (2019) 124894, https://doi.org/10.1016/j.surfcoat.2019.124894.

[12] S.V. Didziulis, K.D. Butcher, A perspective on the properties and surface reactivities of carbides and nitrides of titanium and vanadium, Coord. Chem. Rev. 257 (1) (2013) 93–109, https://doi.org/10.1016/j.ccr.2012.04.015.

[13] E. Kroke, M. Schwarz, Novel group 14 nitrides, Coord. Chem. Rev. 248 (2004) 493–532, https://doi.org/10.1016/j.ccr.2004.02.001.

[14] R.C. Dante, C.K. Kajdas, A review and a fundamental theory of silicon nitride tribochemistry, Wear. 288 (2012) 27–38, https://doi.org/10.1016/j.wear.2012.03.001.

[15] X. Duan, Z. Yang, L. Chen, Z. Tian, D. Cai, Y. Wang, D. Jia, Y.u. Zhou, Review on the properties of hexagonal boron nitride matrix composite ceramics, J. Eur. Ceram. Soc. 36 (15) (2016) 3725–3737, https://doi.org/10.1016/j.jeurceramsoc.2016.05.007.

[16] X.-F. Jiang, Q. Weng, X.-B. Wang, X. Li, J. Zhang, D. Golberg, Y. Bando, Recent Progress on Fabrications and Applications of Boron Nitride Nanomaterials: A Review, J. Mater. Sci. Technol. 31 (6) (2015) 589–598, https://doi.org/10.1016/j.jmst.2014.12.008.

[17] J.I. Pankove, GaN: From fundamentals to applications, Mater. Sci. Eng. B. 61–62 (1999) 305–309, https://doi.org/10.1016/S0921-5107(98)00523-6.

[18] R. Dylewicz, S.Z. Patela, R. Paszkiewicz, Applications of GaN-based materials in modern optoelectronics, in: Proc. SPIE 5484, Photonics Applications in Astronomy, Communications, Industry, and High-Energy Physics Experiments II, 2004: pp. 328–335. https://doi.org/10.1117/12.568864.

[19] P. Chen, Z. Xiong, J. Luo, J. Lin, K, Lee Tan, Interaction of hydrogen with metal nitrides and imides, Nature. 420 (2002) 302–304, https://doi.org/10.1038/nature01210.

[20] N. Tapia-Ruiz, A.G. Gordon, C.M. Jewell, H.K. Edwards, C.W. Dunnill, J.M. Blackman, C.P. Snape, P.D. Brown, I. Maclaren, M. Baldoni, E. Besley, J.J. Titman, D.H. Gregory, Low dimensional nanostructures of fast ion conducting lithium nitride, Nat. Commun. 11 (2020) 4492, https://doi.org/10.1038/s41467-020-17951-6.

[21] T. Shodai, S. Okada, S. Tobishima, J. Yamaki, Anode performance of a new layered nitride $Li_{3-x}Co_xN$ (x = 0.2-0.6), J. Power Sources. 68 (2) (1997) 515–518, https://doi.org/10.1016/S0378-7753(97)02597-4.

[22] K. Chen, R. Pathak, A. Gurung, E.A. Adhamash, B. Bahrami, Q. He, H. Qiao, A.L. Smirnova, J.J. Wu, Q. Qiao, Y. Zhou, Flower-shaped lithium nitride as a protective layer via facile plasma activation for stable lithium metal anodes, Energy Storage Mater. 18 (2019) 389–396, https://doi.org/10.1016/j.ensm.2019.02.006.

[23] J. Choi, E.G. Gillan, Solvothermal Synthesis of Nanocrystalline Copper Nitride from an Energetically Unstable Copper Azide Precursor, Inorg. Chem. 44 (21) (2005) 7385–7393, https://doi.org/10.1021/ic050497j.

[24] G. Paniconi, Z. Stoeva, H. Doberstein, R.I. Smith, B.L. Gallagher, D.H. Gregory, Structural chemistry of Cu_3N powders obtained by ammonolysis reactions, Solid State Sci. 9 (10) (2007) 907–913, https://doi.org/10.1016/j.solidstatesciences.2007.03.017.

[25] H. Jacobs, U. Zachwieja, Kupferpalladiumnitride, Cu_3Pd_xN mit x = 0,020 und 0,989, Perowskite mit "bindender $3d^{10}$-$4d^{10}$-Wechselwirkung", J. Less-Common Met. 170 (1) (1991) 185–190, https://doi.org/10.1016/0022-5088(91)90063-A.

[26] F. Gulo, A. Simon, J. Köhler, R.K. Kremer, Li–Cu Exchange in Intercalated Cu_3N—With a Remark on Cu_4N, Angew. Chemie Int. Ed. 43 (15) (2004) 2032–2034, https://doi.org/10.1002/(ISSN)1521-377310.1002/anie.v43:1510.1002/anie.200353424.

[27] M.G. Moreno-Armenta, A. Martínez-Ruiz, N. Takeuchi, Ab initio total energy calculations of copper nitride: the effect of lattice parameters and Cu content in the electronic properties, Solid State Sci. 6 (1) (2004) 9–14, https://doi.org/10.1016/j.solidstatesciences.2003.10.014.

[28] U. Hahn, W. Weber, Electronic structure and chemical-bonding mechanism of Cu_3N, Cu_3NPd, and related Cu(I) compounds, Phys. Rev. B. 53 (1996) 12684–12693, https://doi.org/10.1103/PhysRevB.53.12684.

[29] C.M. Caskey, R.M. Richards, D.S. Ginley, A. Zakutayev, Thin film synthesis and properties of copper nitride, a metastable semiconductor, Mater. Horizons. 1 (4) (2014) 424–430, https://doi.org/10.1039/C4MH00049H.

[30] X.Y. Cui, A. Soon, A.E. Phillips, R.K. Zheng, Z.W. Liu, B. Delley, S.P. Ringer, C. Stampfl, First principles study of 3*d* transition metal doped Cu_3N, J. Magn. Magn. Mater. 324 (2012) 3138–3143, https://doi.org/10.1016/j.jmmm.2012.05.021.

[31] R. Cremer, M. Witthaut, D. Neuschutz, C. Trappe, M. Laurenzis, O. Winkler, H. Kurz, Deposition and Characterization of Metastable Cu_3N Layers for Applications in Optical Data Storage, Mikrochim. Acta. 133 (1-4) (2000) 299–302, https://doi.org/10.1007/s006040070109.

[32] Z. Ji, Y. Zhang, Y. Yuan, C. Wang, Reactive DC magnetron deposition of copper nitride films for write-once optical recording, Mater. Lett. 60 (29-30) (2006) 3758–3760, https://doi.org/10.1016/j.matlet.2006.03.107.

[33] D.M. Borsa, S. Grachev, C. Presura, D.O. Boerma, Growth and properties of Cu_3N films and Cu_3N/γ'-Fe_4N bilayers, Appl. Phys. Lett. 80 (10) (2002) 1823–1825, https://doi.org/10.1063/1.1459116.

[34] A. Zakutayev, Design of nitride semiconductors for solar energy conversion, J. Mater. Chem. A. 4 (18) (2016) 6742–6754, https://doi.org/10.1039/C5TA09446A.

[35] T. Nosaka, M. Yoshitake, A. Okamoto, S. Ogawa, Y. Nakayama, Thermal decomposition of copper nitride thin films and dots formation by electron beam writing, Appl. Surf. Sci. 169–170 (2001) 358–361, https://doi.org/10.1016/S0169-4332(00)00681-4.

[36] X. Xu, N. Yuan, J. Qiu, J. Ding, Formation of conductive copper lines by femtosecond laser irradiation of copper nitride film on plastic substrates, Mater. Res. Bull. 65 (2015) 68–72, https://doi.org/10.1016/j.materresbull.2015.01.029.

[37] G.H. Yue, P.X. Yan, J.Z. Liu, M.X. Wang, M. Li, X.M. Yuan, Copper nitride thin film prepared by reactive radio-frequency magnetron sputtering, J. Appl. Phys. 98 (10) (2005) 103506, https://doi.org/10.1063/1.2132507.

[38] K. Joo Kim, J. Hyuk Kim, J. Hoon Kang, Structural and optical characterization of Cu_3N films prepared by reactive RF magnetron sputtering, J. Cryst. Growth. 222 (4) (2001) 767–772, https://doi.org/10.1016/S0022-0248(00)00968-4.

[39] Z.Q. Liu, W.J. Wang, T.M. Wang, S. Chao, S.K. Zheng, Thermal stability of copper nitride films prepared by rf magnetron sputtering, Thin Solid Films. 325 (1-2) (1998) 55–59, https://doi.org/10.1016/S0040-6090(98)00448-9.

[40] Y. Du, A.L. Ji, L.B. Ma, Y.Q. Wang, Z.X. Cao, Electrical conductivity and photoreflectance of nanocrystalline copper nitride thin films deposited at low temperature, J. Cryst. Growth. 280 (3-4) (2005) 490–494, https://doi.org/10.1016/j.jcrysgro.2005.03.077.

[41] L. Maya, Deposition of crystalline binary nitride films of tin, copper, and nickel by reactive sputtering, J. Vac. Sci. Technol. A. 11 (3) (1993) 604–608, https://doi.org/10.1116/1.578778.

[42] T. Nosaka, M. Yoshitake, A. Okamoto, S. Ogawa, Y. Nakayama, Copper nitride thin films prepared by reactive radio-frequency magnetron sputtering, Thin Solid Films. 348 (1-2) (1999) 8–13, https://doi.org/10.1016/S0040-6090(98)01776-3.

[43] C. Gallardo-Vega, W. de la Cruz, Study of the structure and electrical properties of the copper nitride thin films deposited by pulsed laser deposition, Appl. Surf. Sci. 252 (22) (2006) 8001–8004, https://doi.org/10.1016/j.apsusc.2005.10.007.

[44] G. Soto, J.A. Díaz, W. de la Cruz, Copper nitride films produced by reactive pulsed laser deposition, Mater. Lett. 57 (26-27) (2003) 4130–4133, https://doi.org/10.1016/S0167-577X(03)00277-5.

[45] D.M. Borsa, D.O. Boerma, Growth, structural and optical properties of Cu_3N films, Surf. Sci. 548 (1-3) (2004) 95–105, https://doi.org/10.1016/j.susc.2003.10.053.

[46] J.M. Park, K. Jin, B. Han, M.J. Kim, J. Jung, J.J. Kim, W.J. Lee, Atomic layer deposition of copper nitride film and its application to copper seed layer for electrodeposition, Thin Solid Films. 556 (2014) 434–439, https://doi.org/10.1016/j.tsf.2014.01.034.

[47] M. Asano, K. Umeda, A. Tasaki, Cu_3N Thin Film for a New Light Recording Media, Jpn. J. Appl. Phys. 29 (Part 1, No. 10) (1990) 1985–1986.

[48] N. Gordillo, R. Gonzalez-Arrabal, M.S. Martin-Gonzalez, J. Olivares, A. Rivera, F. Briones, F. Agulló-López, D.O. Boerma, DC triode sputtering deposition and characterization of N-rich copper nitride thin films: Role of chemical composition, J. Cryst. Growth. 310 (19) (2008) 4362–4367, https://doi.org/10.1016/j.jcrysgro.2008.07.051.

[49] K. Venkata Subba Reddy, A. Sivasankar Reddy, P. Sreedhara Reddy, S. Uthanna, Copper nitride films deposited by dc reactive magnetron sputtering, J. Mater. Sci. Mater. Electron. 18 (10) (2007) 1003–1008, https://doi.org/10.1007/s10854-007-9120-0.

[50] R. Gonzalez-Arrabal, N. Gordillo, M.S. Martin-Gonzalez, R. Ruiz-Bustos, F. Agulló-López, Thermal stability of copper nitride thin films: The role of nitrogen migration, J. Appl. Phys. 107 (10) (2010) 103513, https://doi.org/10.1063/1.3369450.

[51] Q. Lu, X. Zhang, W. Zhu, Y. Zhou, Q. Zhou, L. Liu, X. Wu, Reproducible resistive-switching behavior in copper-nitride thin film prepared by plasma-immersion ion implantation, Phys. Status Solidi. 208 (4) (2011) 874–877, https://doi.org/10.1002/pssa.201026680.

[52] D. Wang, N. Nakamine, Y. Hayashi, Properties of various sputter-deposited Cu–N thin films, J. Vac. Sci. Technol. A. 16 (4) (1998) 2084–2092.

[53] A. Jiang, M. Qi, J. Xiao, Preparation, structure, properties, and application of copper nitride (Cu_3N) thin films: A review, J. Mater. Sci. Technol. 34 (9) (2018) 1467–1473, https://doi.org/10.1016/j.jmst.2018.02.025.

[54] R. Juza, H. Hahn, Über die Kristallstrukturen von Cu3N, GaN und InN, Z. Anorg. Allg. Chem. 239 (1938) 282–287.

[55] H. Wu, W. Chen, Copper Nitride Nanocubes: Size-Controlled Synthesis and Application as Cathode Catalyst in Alkaline Fuel Cells, J. Am. Chem. Soc. 133 (39) (2011) 15236–15239, https://doi.org/10.1021/ja204748u.

[56] T. Nakamura, H. Hayashi, T. Hanaoka, T. Ebina, Preparation of Copper Nitride (Cu_3N) Nanoparticles in Long-Chain Alcohols at 130–200 °C and Nitridation Mechanism, Inorg. Chem. 53 (2) (2014) 710–715, https://doi.org/10.1021/ic4011604.

[57] N. Pereira, L. Dupont, J.M. Tarascon, L.C. Klein, G.G. Amatucci, Electrochemistry of Cu_3N with Lithium A Complex System with Parallel Processes, J. Electrochem. Soc. 150 (2003) A1273–A1280, https://doi.org/10.1149/1.1599845.

[58] R. Deshmukh, G. Zeng, E. Tervoort, M. Staniuk, D. Wood, M. Niederberger, Ultrasmall Cu_3N Nanoparticles: Surfactant-Free Solution-Phase Synthesis, Nitridation Mechanism, and Application for Lithium Storage, Chem. Mater. 27 (24) (2015) 8282–8288, https://doi.org/10.1021/acs.chemmater.5b0344410.1021/acs.chemmater.5b03444.s001.

[59] D.D. Vaughn II, J. Araujo, P. Meduri, J.F. Callejas, M.A. Hickner, R.E. Schaak, Solution Synthesis of Cu_3PdN Nanocrystals as Ternary Metal Nitride Electrocatalysts for the Oxygen Reduction Reaction, Chem. Mater. 26 (21) (2014) 6226–6232, https://doi.org/10.1021/cm5029723.

[60] Y.-R. Luo, Comprehensive Handbook of Chemical Bond Energies, CRC Press, Boca Raton, 2007, https://doi.org/https://doi.org/10.1201/9781420007282.

[61] W. Sun, A. Holder, B. Orvañanos, E. Arca, A. Zakutayev, S. Lany, G. Ceder, Thermodynamic Routes to Novel Metastable Nitrogen-Rich Nitrides, Chem. Mater. 29 (16) (2017) 6936–6946, https://doi.org/10.1021/acs.chemmater.7b0239910.1021/acs.chemmater.7b02399.s001.

[62] R. Juza, H. Hahn, Kupfernitrid, Z. Anorg. Allg. Chem. 241 (1939) 172–178.

[63] B.S. Lee, M. Yi, S.Y. Chu, J.Y. Lee, H.R. Kwon, K.R. Lee, D. Kang, W.S. Kim, H. Bin Lim, J. Lee, H.J. Youn, D.Y. Chi, N.H. Hur, Copper nitride nanoparticles supported on a superparamagnetic mesoporous microsphere for toxic-free click chemistry, Chem. Commun. 46 (2010) 3935–3937, https://doi.org/10.1039/c001255f.

[64] R. Szczęsny, E. Szłyk, M.A. Wiśniewski, T.K.A. Hoang, D.H. Gregory, Facile preparation of copper nitride powders and nanostructured films, J. Mater. Chem. C. 4 (22) (2016) 5031–5037, https://doi.org/10.1039/C6TC00493H.

[65] R. Deshmukh, U. Schubert, Synthesis of CuO and Cu_3N Nanoparticles in and on Hollow Silica Spheres, Eur. J. Inorg. Chem. 2013 (14) (2013) 2498–2504, https://doi.org/10.1002/ejic.201201442.

[66] M.D. Reichert, M.A. White, M.J. Thompson, G.J. Miller, J. Vela, Preparation and Instability of Nanocrystalline Cuprous Nitride, Inorg. Chem. 54 (13) (2015) 6356–6362, https://doi.org/10.1021/acs.inorgchem.5b00679.

[67] X. Li, A.L. Hector, J.R. Owen, Evaluation of Cu_3N and CuO as Negative Electrode Materials for Sodium Batteries, J. Phys. Chem. C. 118 (51) (2014) 29568–29573, https://doi.org/10.1021/jp509385w.

[68] A. Baiker, M. Maciejewski, Formation and thermal stability of copper and nickel nitrides, J. Chem. Soc. Faraday Trans. 1 (80) (1984) 2331–2341, https://doi.org/10.1039/F19848002331.

[69] E.C. Franklin, The action of potassium amide on cupric nitrate in liquid ammonia solution. (cuprous imide, cuprous nitride and potassium ammonocuprite.), J. Am. Chem. Soc. 34 (1912) 1501–1507, https://doi.org/10.1021/ja02212a010.

[70] U. Zachwieja, H. Jacobs, Ammonothermalsynthese von kupfernitrid, Cu_3N, J. Less-Common Met. 161 (1) (1990) 175–184, https://doi.org/10.1016/0022-5088(90)90327-G.

[71] R.I. Walton, Subcritical solvothermal synthesis of condensed inorganic materials, Chem. Soc. Rev. 31 (2002) 230–238, https://doi.org/10.1039/b105762f.

[72] T.M.M. Richter, R. Niewa, Chemistry of Ammonothermal Synthesis, Inorganics. 2 (2014) 29–78, https://doi.org/10.3390/inorganics2010029.

[73] L. Haar, J.S. Gallagher, Thermodynamic properties of ammonia, J. Phys. Chem. Ref. Data. 7 (3) (1978) 635–792, https://doi.org/10.1063/1.555579.

[74] S. Desmoulins-Krawiec, C. Aymonier, A. Loppinet-Serani, F. Weill, S. Gorsse, J. Etourneau, F. Cansell, Synthesis of nanostructured materials in supercritical ammonia: nitrides, metals and oxides, J. Mater. Chem. 14 (2004) 228–232, https://doi.org/10.1039/b310806f.

[75] S.A. Rasaki, B. Zhang, K. Anbalgam, T. Thomas, M. Yang, Synthesis and application of nano-structured metal nitrides and carbides: A review, Prog. Solid State Chem. 50 (2018) 1–15, https://doi.org/10.1016/j.progsolidstchem.2018.05.001.

[76] B. Mazumder, P. Chirico, A.L. Hector, Direct Solvothermal Synthesis of Early Transition Metal Nitrides, Inorg. Chem. 47 (20) (2008) 9684–9690, https://doi.org/10.1021/ic800767m.

[77] D. Wang, Y. Li, Controllable synthesis of Cu-based nanocrystals in ODA solvent, Chem. Commun. 47 (2011) 3604–3606, https://doi.org/10.1039/c0cc04902f.

[78] P. Xi, Z. Xu, D. Gao, F. Chen, D. Xue, C.-L. Tao, Z.-N. Chen, Solvothermal synthesis of magnetic copper nitride nanocubes with highly electrocatalytic reduction properties, RSC Adv. 4 (27) (2014) 14206–14209, https://doi.org/10.1039/C4RA01307G.

[79] Z. Yin, C. Yu, Z. Zhao, X. Guo, M. Shen, N. Li, M. Muzzio, J. Li, H. Liu, H. Lin, J. Yin, G. Lu, D. Su, S. Sun, Cu_3N Nanocubes for Selective Electrochemical Reduction of CO_2 to Ethylene, Nano Lett. 19 (12) (2019) 8658–8663, https://doi.org/10.1021/acs.nanolett.9b0332410.1021/acs.nanolett.9b03324.s001.

[80] D. Barman, S. Paul, S. Ghosh, S.K. De, Cu_3N Nanocrystals Decorated with Au Nanoparticles for Photocatalytic Degradation of Organic Dyes, ACS Appl. Nano Mater. 2 (8) (2019) 5009–5019, https://doi.org/10.1021/acsanm.9b0094310.1021/acsanm.9b00943.s001.

[81] R.K. Sithole, L.F.E. MacHogo, M.A. Airo, S.S. Gqoba, M.J. Moloto, P. Shumbula, J. Van Wyk, N. Moloto, Synthesis and characterization of Cu_3N nanoparticles using pyrrole-2-carbaldpropyliminato Cu(II) complex and $Cu(NO_3)_2$ as single-source precursors: the search for an ideal precursor, New J. Chem. 42 (2018) 3042–3049, https://doi.org/10.1039/c7nj05181f.

[82] R.K. Sithole, T. Kolokoto, L.F.E. Machogo, G.N. Ngubeni, M.J. Moloto, J. Van Wyk, N. Moloto, Simultaneous capping and substitution of nitrogen ions of Cu_3N nanocrystals with sulfur ions using DDT as a co-surfactant to form chalcocite and digenite nanocrystals, Mater. Chem. Phys. 251 (2020) 123074, https://doi.org/10.1016/j.matchemphys.2020.123074.

[83] R.K. Sithole, L.F.E. Machogo, M.J. Moloto, S.S. Gqoba, K.P. Mubiayi, J. Van Wyk, N. Moloto, One-step synthesis of Cu_3N, Cu_2S and Cu_9S_5 and photocatalytic degradation of methyl orange and methylene blue, J. Photochem. Photobiol. A Chem. 397 (2020) 112577, https://doi.org/10.1016/j.jphotochem.2020.112577.

[84] R. Kadzutu-Sithole, L.F.E. Machogo-Phao, T. Kolokoto, M. Zimuwandeyi, S.S. Gqoba, K.P. Mubiayi, M.J. Moloto, J. Van Wyk, N. Moloto, Elucidating the effect of precursor decomposition time on the structural and optical properties of copper(I) nitride nanocubes, RSC Adv. 10 (2020) 34231–34246, https://doi.org/10.1039/c9ra09546b.

[85] A. Miura, T. Takei, N. Kumada, Synthesis of Cu_3N from CuO and $NaNH_2$, J. Asian Ceram. Soc. 2 (4) (2014) 326–328, https://doi.org/10.1016/j.jascer.2014.08.007.

[86] R. Deshmukh, E. Tervoort, J. Käch, F. Rechberger, M. Niederberger, Assembly of ultrasmall Cu_3N nanoparticles into three-dimensional porous monolithic aerogels, Dalt. Trans. 45 (29) (2016) 11616–11619, https://doi.org/10.1039/C6DT01451H.

[87] S. Mondal, C.R. Raj, Copper Nitride Nanostructure for the Electrocatalytic Reduction of Oxygen: Kinetics and Reaction Pathway, J. Phys. Chem. C. 122 (32) (2018) 18468–18475, https://doi.org/10.1021/acs.jpcc.8b0384010.1021/acs.jpcc.8b03840.s001.

[88] T. Nakamura, H. Hayashi, T. Ebina, Preparation of copper nitride nanoparticles using urea as a nitrogen source in a long-chain alcohol, J. Nanoparticle Res. 16 (2014) 1–6, https://doi.org/10.1007/s11051-014-2699-1.

[89] T. Nakamura, Influence of Fatty Acid Alkyl Chain Length on Anisotropy of Copper Nitride Nano-Crystallites, Inorganics. 5 (2017) 6, https://doi.org/10.3390/inorganics5010006.

[90] A. Egeberg, L. Warmuth, S. Riegsinger, D. Gerthsen, C. Feldmann, Pyridine-based low-temperature synthesis of CoN, Ni_3N and Cu_3N nanoparticles, Chem. Commun. 54 (71) (2018) 9957–9960, https://doi.org/10.1039/C8CC04893B.

[91] S. Li, W. Cheng, L. Yan, C. Xu, N. Zhu, Z. Zhang, W. Li, S. Yu, Synthesis and formation mechanism of pyramidal Cu_3N microcrystal in supercritical fluids, Inorg. Nano-Metal Chem. 49 (2) (2019) 51–55, https://doi.org/10.1080/24701556.2019.1599399.

[92] N. Kieda, G.L. Messing, Microfoamy particles of copper oxide and nitride by spray pyrolysis of copper-ammine complex solutions, J. Mater. Sci. Lett. 17 (1998) 299–301, https://doi.org/10.1023/A:1006581605833.

[93] C. Panda, P.W. Menezes, M. Zheng, S. Orthmann, M. Driess, In Situ Formation of Nanostructured Core-Shell Cu_3N-CuO to Promote Alkaline Water Electrolysis, ACS Energy Lett. 4 (3) (2019) 747–754, https://doi.org/10.1021/acsenergylett.9b0009110.1021/acsenergylett.9b00091.s001.

[94] I.P. Parkin, Solid state metathesis reaction for metal borides, silicides, pnictides and chalcogenides: ionic or elemental pathways, Chem. Soc. Rev. 25 (1996) 199–207, https://doi.org/10.1039/cs9962500199.

[95] S. Dong, X. Chen, X. Zhang, G. Cui, Nanostructured transition metal nitrides for energy storage and fuel cells, Coord. Chem. Rev. 257 (13-14) (2013) 1946–1956, https://doi.org/10.1016/j.ccr.2012.12.012.

[96] C. Cohen, H. Ellmer, J.M. Guigner, A. L'Hoir, G. Prévot, D. Schmaus, M. Sotto, Surface relaxation and near-surface atomic displacements in the N/Cu(100) self-ordered system, Surf. Sci. 490 (3) (2001) 336–350, https://doi.org/10.1016/S0039-6028(01)01353-X.

[97] F.M. Leibsle, C.F.J. Flipse, A.W. Robinson, Structure of the Cu{100}-c(2×2)N surface: A scanning-tunneling-microscopy study, Phys. Rev. B. 47 (23) (1993) 15865–15868, https://doi.org/10.1103/PhysRevB.47.15865.

[98] D. Heskett, A. Baddorf, E.W. Plummer, Nitrogen-induced reconstruction of Cu (110): Formation of a surface nitride, Surf. Sci. 195 (1-2) (1988) 94–102, https://doi.org/10.1016/0039-6028(88)90782-0.

[99] G.G. Tibbetts, J.M. Burkstrand, J.C. Tracy, Electronic properties of adsorbed layers of nitrogen, oxygen, and sulfur on copper (100), Phys. Rev. B. 15 (8) (1977) 3652–3660, https://doi.org/10.1103/PhysRevB.15.3652.

[100] S.M. Driver, D.P. Woodruff, Nitrogen-induced pseudo-(100) reconstruction of the Cu(111) surface identified by STM, Surf. Sci. 442 (1) (1999) 1–8, https://doi.org/10.1016/S0039-6028(99)00906-1.

[101] R.N. Lee, H.E. Farnsworth, LEED studies of adsorption on clean (100) copper surfaces, Surf. Sci. 3 (5) (1965) 461–479, https://doi.org/10.1016/0039-6028(65)90026-9.

[102] G.G. Tibbetts, Electronically activated chemisorption of nitrogen on a copper (100) surface, J. Chem. Phys. 70 (8) (1979) 3600–3603, https://doi.org/10.1063/1.437963.

[103] J.M. Burkstrand, G.G. Kleiman, G.G. Tibbetts, J.C. Tracy, Study of the N-Cu (100) system, J. Vac. Sci. Technol. 13 (1) (1976) 291–295, https://doi.org/10.1116/1.568830.

[104] G.G. Kleiman, J.M. Burkstrand, An objective approach for deriving surface structure: Application to Cu(100)/N, Solid State Commun. 21 (1) (1977) 5–8, https://doi.org/10.1016/0038-1098(77)91466-1.

[105] H.C. Zeng, R.N.S. Sodhi, K.A.R. Mitchell, A leed crystallographic analysis for the Cu(100)c(2×2)-N surface structure, Surf. Sci. 188 (3) (1987) 599–608.

[106] D.T. Vu Grimsby, M.Y. Zhou, K.A.R. Mitchell, LEED crystallographic studies for the Cu(110)-(2×3)-N surface structure, Surf. Sci. 271 (3) (1992) 519–529, https://doi.org/10.1016/0039-6028(92)90913-Q.

[107] A. Soon, L. Wong, B. Delley, C. Stampfl, Morphology of copper nanoparticles in a nitrogen atmosphere: A first-principles investigation, Phys. Rev. B. 77 (2008), https://doi.org/10.1103/PhysRevB.77.125423 125423.

[108] T. Choi, C.D. Ruggiero, J.A. Gupta, Incommensurability and atomic structure of c(2×2)N/Cu(100): A scanning tunneling microscopy study, Phys. Rev. B. 78 (2008), https://doi.org/10.1103/PhysRevB.78.035430 035430.

[109] D. Écija, J.M. Gallego, R. Miranda, The adsorption of atomic N and the growth of copper nitrides on Cu(100), Surf. Sci. 603 (15) (2009) 2283–2289, https://doi.org/10.1016/j.susc.2009.04.039.

[110] M. Ohring, The Materials Science of Thin Films, Academic Press, San Diego, 1992.

[111] S. Terada, H. Tanaka, K. Kubota, Heteroepitaxial growth of Cu_3N thin films, J. Cryst. Growth. 94 (2) (1989) 567–568, https://doi.org/10.1016/0022-0248(89)90038-9.

[112] A. von Richthofen, R. Domnick, R. Cremer, Cu-N Films Grown by Reactive MSIP: Constitution, Structure and Morphology, Mikrochim. Acta. 125 (1-4) (1997) 173–177, https://doi.org/10.1007/BF01246182.

[113] I.M. Odeh, Fabrication and optical constants of amorphous copper nitride thin films prepared by ion beam assisted dc magnetron reactive sputtering, J. Alloys Compd. 454 (1-2) (2008) 102–105, https://doi.org/10.1016/j.jallcom.2006.12.020.

[114] T. Maruyama, T. Morishita, Copper nitride thin films prepared by radio-frequency reactive sputtering, J. Appl. Phys. 78 (6) (1995) 4104–4107, https://doi.org/10.1063/1.359868.

[115] X.M. Yuan, P.X. Yan, J.Z. Liu, Preparation and characterization of copper nitride films at various nitrogen contents by reactive radio-frequency magnetron sputtering, Mater. Lett. 60 (15) (2006) 1809–1812, https://doi.org/10.1016/j.matlet.2005.12.028.

[116] G.H. Yue, P.X. Yan, J. Wang, Study on the preparation and properties of copper nitride thin films, J. Cryst. Growth. 274 (3-4) (2005) 464–468, https://doi.org/10.1016/j.jcrysgro.2004.10.032.
[117] G.H. Yue, J.Z. Liu, M. Li, X.M. Yuan, P.X. Yan, J.L. Liu, Hall effect of copper nitride thin films, Phys. Status Solidi A. 202 (10) (2005) 1987–1993, https://doi.org/10.1002/(ISSN)1521-396X10.1002/pssa:v202:1010.1002/pssa:200420062.
[118] S. Ghosh, F. Singh, D. Choudhary, D.K. Avasthi, V. Ganesan, P. Shah, A. Gupta, Effect of substrate temperature on the physical properties of copper nitride films by r.f. reactive sputtering, Surf. Coat. Technol. 142–144 (2001) 1034–1039, https://doi.org/10.1016/S0257-8972(01)01091-X.
[119] J. Wang, J.T. Chen, X.M. Yuan, Z.G. Wu, B.B. Miao, P.X. Yan, Copper nitride (Cu_3N) thin films deposited by RF magnetron sputtering, J. Cryst. Growth. 286 (2) (2006) 407–412, https://doi.org/10.1016/j.jcrysgro.2005.10.107.
[120] J.F. Pierson, Structure and properties of copper nitride films formed by reactive magnetron sputtering, Vacuum. 66 (1) (2002) 59–64, https://doi.org/10.1016/S0042-207X(01)00425-0.
[121] J.F. Pierson, D. Wiederkehr, A. Billard, Reactive magnetron sputtering of copper, silver, and gold, Thin Solid Films. 478 (1-2) (2005) 196–205, https://doi.org/10.1016/j.tsf.2004.10.043.
[122] X. Li, Q. Bai, J. Yang, Y. Li, L. Wang, H. Wang, S. Ren, S. Liu, W. Huang, Effect of N_2-gas flow rates on the structures and properties of copper nitride films prepared by reactive DC magnetron sputtering, Vacuum. 89 (2013) 78–81, https://doi.org/10.1016/j.vacuum.2011.10.020.
[123] S. Swann, Magnetron sputtering, Phys. Technol. 19 (2) (1988) 67–75, https://doi.org/10.1088/0305-4624/19/2/304.
[124] L. Soukup, M. Šícha, F. Fendrych, L. Jastrabík, Z. Hubička, D. Chvostová, H. Šíchová, V. Valvoda, A. Tarasenko, V. Studnička, T. Wagner, M. Novák, Copper nitride thin films prepared by the RF plasma chemical reactor with low pressure supersonic single and multi-plasma jet system, Surf. Coat. Technol. 116–119 (1999) 321–326, https://doi.org/10.1016/S0257-8972(99)00129-2.
[125] F. Fendrych, L. Soukup, L. Jastrabık, M. Šicha, Z. Hubička, D. Chvostová, A. Tarasenko, V. Studnička, T. Wagner, Cu_3N films prepared by the low-pressure r.f. supersonic plasma jet reactor: Structure and optical properties, Diam. Relat. Mater. 8 (8-9) (1999) 1715–1719, https://doi.org/10.1016/S0925-9635(99)00063-1.
[126] R. Miyano, K. Kimura, K. Izumi, H. Takikawa, T. Sakakibara, Preparation of metal nitride and oxide thin films using shielded reactive vacuum arc deposition, Vacuum. 59 (1) (2000) 159–167, https://doi.org/10.1016/S0042-207X(00)00266-9.
[127] J. Pinkas, J.C. Huffman, D.V. Baxter, M.H. Chisholm, K.G. Caulton, Mechanistic Role of H_2O and the Ligand in the Chemical Vapor Deposition of Cu, Cu_2O, CuO, and Cu_3N from Bis (1,1,1,5,5,5-hexafluoropentane-2,4-dionato) copper (II), Chem. Mater. 7 (8) (1995) 1589–1596, https://doi.org/10.1021/cm00056a028.
[128] A. Fallberg, M. Ottosson, J.O. Carlsson, CVD of Copper(I) Nitride, Chem. Vap. Depos. 15 (2009) 300–305, https://doi.org/10.1002/cvde.200906794.
[129] A. Modin, K.O. Kvashnina, S.M. Butorin, L. Werme, J. Nordgren, S. Arapan, R. Ahuja, A. Fallberg, M. Ottosson, Electronic structure of Cu_3N films studied by soft x-ray spectroscopy, J. Phys. Condens. Matter. 20 (23) (2008) 235212, https://doi.org/10.1088/0953-8984/20/23/235212.
[130] S.O. Kucheyev, J. Biener, T.F. Baumann, Y.M. Wang, A.V. Hamza, Z. Li, D.K. Lee, R.G. Gordon, Mechanisms of Atomic Layer Deposition on Substrates with Ultrahigh Aspect Ratios, Langmuir. 24 (3) (2008) 943–948, https://doi.org/10.1021/la7018617.
[131] Z. Li, R.G. Gordon, Thin, continuous, and conformal copper films by reduction of atomic layer deposited copper nitride, Chem. Vap. Depos. 12 (7) (2006) 435–441, https://doi.org/10.1002/(ISSN)1521-386210.1002/cvde.v12:710.1002/cvde.200606485.
[132] M.N. Terao, Etude par diffraction électronique du nitrure de cuivre Cu_3N, C. R. Académie Des Sci. Paris. 277 (1973) 595–598.
[133] R. Szczęsny, T.M. Muzioł, D.H. Gregory, E. Szłyk, Structural and thermal characterization of copper(II) complexes with phenyl-2-pyridylketoxime and deposition of thin films by spin coating, Chem. Pap. 69 (2015) 569–579, https://doi.org/10.1515/chempap-2015-0065.
[134] Z. Wang, X. Cao, D. Liu, S. Hao, R. Kong, G. Du, A.M. Asiri, X. Sun, Copper-Nitride Nanowires Array: An Efficient Dual-Functional Catalyst Electrode for Sensitive and Selective Non-Enzymatic Glucose and Hydrogen Peroxide Sensing, Chem. Eur. J. 23 (21) (2017) 4986–4989, https://doi.org/10.1002/chem.201700366.
[135] F.-L. Meng, H.-X. Zhong, Q. Zhang, K.-H. Liu, J.-M. Yan, Q. Jiang, Integrated Cu_3N porous nanowire array electrode for high-performance supercapacitors, J. Mater. Chem. A. 5 (36) (2017) 18972–18976, https://doi.org/10.1039/C7TA05439D.
[136] J. Li, X. Kong, M. Jiang, X. Lei, Hierarchically structured CoN/Cu_3N nanotube array supported on copper foam as an efficient bifunctional electrocatalyst for overall water splitting, Inorg. Chem. Front. 5 (11) (2018) 2906–2913, https://doi.org/10.1039/C8QI00860D.
[137] X. Zhou, X. Li, D. Chen, D. Zhao, X. Huang, Ultrathin CoFe-layered double hydroxide nanosheets embedded in high conductance Cu_3N nanowire arrays with a 3D core-shell architecture for ultrahigh capacitance supercapacitors, J. Mater. Chem. A. 6 (47) (2018) 24603–24613, https://doi.org/10.1039/C8TA09442J.
[138] A. Scigala, E. Szłyk, T. Rerek, M. Wiśniewski, L. Skowronski, M. Trzcinski, R. Szczesny, Copper Nitride Nanowire Arrays—Comparison of Synthetic Approaches, Materials 14 (2021), https://doi.org/10.3390/ma14030603, In press.
[139] K. Nowakowska-Langier, R. Chodun, R. Minikayev, S. Okrasa, G.W. Strzelecki, B. Wicher, K. Zdunek, Phase composition of copper nitride coatings examined by the use of X-ray diffraction and Raman spectroscopy, J. Mol. Struct. 1165 (2018) 79–83, https://doi.org/10.1016/j.molstruc.2018.03.107.
[140] A. Zakutayev, C.M. Caskey, A.N. Fioretti, D.S. Ginley, J. Vidal, V. Stevanovic, E. Tea, S. Lany, Defect Tolerant Semiconductors for Solar Energy Conversion, J. Phys. Chem. Lett. 5 (7) (2014) 1117–1125, https://doi.org/10.1021/jz5001787.
[141] J. Wang, F. Li, X. Liu, H. Zhou, X. Shao, Y. Qu, M. Zhao, Cu_3N and its analogs: a new class of electrodes for lithium ion batteries, J. Mater. Chem. A. 5 (18) (2017) 8762–8768, https://doi.org/10.1039/C7TA02339A.
[142] M. Zervos, A. Othonos, M. Sergides, T. Pavloudis, J. Kioseoglou, Observation of the Direct Energy Band Gaps of Defect-Tolerant Cu3N by Ultrafast Pump-Probe Spectroscopy, J. Phys. Chem. C. 124 (6) (2020) 3459–3469, https://doi.org/10.1021/acs.jpcc.9b10303.
[143] C. Navío, M.J. Capitán, J. Álvarez, F. Yndurain, R. Miranda, Intrinsic surface band bending in Cu_3N (100) ultrathin films, Phys. Rev. B. 76 (2007), https://doi.org/10.1103/PhysRevB.76.085105 085105.
[144] T. Nakamura, M. Katayama, T. Watanabe, Y. Inada, T. Ebina, A. Yamaguchi, Stability of Copper Nitride Nanoparticles under High Humidity and in Solutions with Different Acidity, Chem. Lett. 44 (6) (2015) 755–757, https://doi.org/10.1246/cl.150128.
[145] T. Maruyama, T. Morishita, Copper nitride and tin nitride thin films for write-once optical recording media, Appl. Phys. Lett. 69 (1996) 890–891. https://doi.org/10.1063/1.117978.
[146] G. Sahoo, S.R. Meher, M.K. Jain, Room temperature growth of high crystalline quality Cu_3N thin films by modified activated reactive evaporation, Mater. Sci. Eng. B. 191 (2015) 7–14, https://doi.org/10.1016/j.mseb.2014.10.002.
[147] L. Maya, Covalent nitrides for maskless laser writing of microscopic metal lines, Mater. Res. Soc. Symp. Proc. 282 (1993) 203–208, https://doi.org/10.1557/proc-282-203.
[148] S.Y. Wang, J.H. Qiu, X.Q. Wang, N.Y. Yuan, J.N. Ding, W.H. Huang, The evolution of Cu_3N films irradiated by femtosecond laser pulses, Appl. Surf. Sci. 268 (2013) 387–390, https://doi.org/10.1016/j.apsusc.2012.12.106.
[149] N. Lesch, P. Karduck, R. Cremer, A.v. Richthofen, Investigation of the electron beam induced transformation of Cu_3N-films, Fresenius J. Anal. Chem. 361 (6-7) (1998) 604–607, https://doi.org/10.1007/s002160050964.
[150] Y. Du, Y. Yin, J. Wang, Z. Wang, C. Li, S. Baunack, L. Ma, O.G. Schmidt, Nanoporous Copper Pattern Fabricated by Electron Beam Irradiation on Cu_3N Film for SERS Application, Phys. Status Solidi B. 256 (2) (2019) 1800378, https://doi.org/10.1002/pssb:v256.210.1002/pssb:201800378.
[151] K. Matsuzaki, T. Katase, T. Kamiya, H. Hosono, Symmetric Ambipolar Thin-Film Transistors and High-Gain CMOS-like Inverters Using Environmentally Friendly Copper Nitride, ACS Appl. Mater. Interfaces. 11 (38) (2019) 35132–35137, https://doi.org/10.1021/acsami.9b1206810.1021/acsami.9b12068.s001.
[152] W. Chen, H. Zhang, B. Yang, B. Li, Z. Li, Characterization of Cu_3N/CuO thin films derived from annealed Cu_3N for electrode application in Li-ion batteries, Thin Solid Films. 672 (2019) 157–164, https://doi.org/10.1016/j.tsf.2019.01.013.
[153] C. Uthaisar, V. Barone, Edge Effects on the Characteristics of Li Diffusion in Graphene, Nano Lett. 10 (8) (2010) 2838–2842, https://doi.org/10.1021/nl100865a.
[154] S.-H. Yu, X. Feng, N. Zhang, J. Seok, Héctor.D. Abruña, Understanding Conversion-Type Electrodes for Lithium Rechargeable Batteries, Acc. Chem. Res. 51 (2) (2018) 273–281, https://doi.org/10.1021/acs.accounts.7b00487.
[155] Y. Sun, G. Zheng, Z.W. Seh, N. Liu, S. Wang, J. Sun, H.R. Lee, Y. Cui, Graphite-Encapsulated Li-Metal Hybrid Anodes for High-Capacity Li Batteries, Chem. 1 (2) (2016) 287–297, https://doi.org/10.1016/j.chempr.2016.07.009.
[156] Y. Liu, D. Lin, P.Y. Yuen, K. Liu, J. Xie, R.H. Dauskardt, Y. Cui, An Artificial Solid Electrolyte Interphase with High Li-Ion Conductivity, Mechanical Strength, and Flexibility for Stable Lithium Metal Anodes, Adv. Mater. 29 (10) (2017) 1605531, https://doi.org/10.1002/adma.201605531.
[157] Q. Li, H. Pan, W. Li, Y. Wang, J. Wang, J. Zheng, X. Yu, H. Li, L. Chen, Homogeneous Interface Conductivity for Lithium Dendrite-Free Anode, ACS Energy Lett. 3 (9) (2018) 2259–2266, https://doi.org/10.1021/acsenergylett.8b0124410.1021/acsenergylett.8b01244.s001.
[158] D. Lee, S. Sun, J. Kwon, H. Park, M. Jang, E. Park, B. Son, Y. Jung, T. Song, U. Paik, Copper Nitride Nanowires Printed Li with Stable Cycling for Li Metal Batteries in Carbonate Electrolytes, Adv. Mater. 32 (7) (2020) 1905573, https://doi.org/10.1002/adma.v32.710.1002/adma.201905573.
[159] H. Park, J. Kwon, T. Song, U. Paik, Lithiophilic surface treatment of metal- and metallic compound-based frameworks by gas nitriding for lithium metal batteries, J. Power Sources. 477 (2020) 228776, https://doi.org/10.1016/j.jpowsour.2020.228776.
[160] Q. Wang, Z. Zhang, X. Zhao, J. Xiao, D. Manoj, F. Wei, F. Xiao, H. Wang, S. Wang, MOF-Derived Copper Nitride/Phosphide Heterostructure Coated by Multi-Doped Carbon as Electrocatalyst for Efficient Water Splitting and Neutral-pH Hydrogen Evolution Reaction, ChemElectroChem. 7 (1) (2020) 289–298, https://doi.org/10.1002/celc.v7.110.1002/celc.201901860.
[161] J. Li, C. Yao, X. Kong, Z. Li, M. Jiang, F. Zhang, X. Lei, Boosting Hydrogen Production by Electrooxidation of Urea over 3D Hierarchical Ni_4N/Cu_3N Nanotube Arrays, ACS Sustain. Chem. Eng. 7 (15) (2019) 13278–13285,

https://doi.org/10.1021/acssuschemeng.9b0251010.1021/acssuschemeng.9b02510.s001.
[162] C.-Y. Su, B.-H. Liu, T.-J. Lin, Y.-M. Chi, C.-C. Kei, K.-W. Wang, T.-P. Perng, Carbon nanotube-supported Cu_3N nanocrystals as a highly active catalyst for oxygen reduction reaction, J. Mater. Chem. A. 3 (37) (2015) 18983–18990, https://doi.org/10.1039/C5TA04383B.
[163] H. Xie, T. Wang, J. Liang, Q. Li, S. Sun, Cu-based nanocatalysts for electrochemical reduction of CO_2, Nano Today. 21 (2018) 41–54, https://doi.org/10.1016/j.nantod.2018.05.001.
[164] Y. Mi, S. Shen, X. Peng, H. Bao, X. Liu, J. Luo, Selective Electroreduction of CO_2 to C2 Products over Cu_3N-Derived Cu Nanowires, ChemElectroChem. 6 (9) (2019) 2393–2397, https://doi.org/10.1002/celc.v6.910.1002/celc.201801826.
[165] Z.Q. Liang, T.T. Zhuang, A. Seifitokaldani, J. Li, C.W. Huang, C.S. Tan, Y. Li, P. De Luna, C.T. Dinh, Y. Hu, Q. Xiao, P.L. Hsieh, Y. Wang, F. Li, R. Quintero-Bermudez, Y. Zhou, P. Chen, Y. Pang, S.C. Lo, L.J. Chen, H. Tan, Z. Xu, S. Zhao, D. Sinton, E.H. Sargent, Copper-on-nitride enhances the stable electrosynthesis of multi-carbon products from CO_2, Nat. Commun. 9 (2018) 3828, https://doi.org/10.1038/s41467-018-06311-0.
[166] F.L.P. Veenstra, A.J. Martín, J. Pérez-Ramírez, Nitride-Derived Copper Modified with Indium as a Selective and Highly Stable Catalyst for the Electroreduction of Carbon Dioxide, ChemSusChem 12 (2019) 3501–3508, https://doi.org/10.1002/cssc.201901309.
[167] A. Zakutayev, A.J. Allen, X. Zhang, J. Vidal, Z. Cui, S. Lany, M. Yang, F.J. DiSalvo, D.S. Ginley, Experimental Synthesis and Properties of Metastable $CuNbN_2$ and Theoretical Extension to Other Ternary Copper Nitrides, Chem. Mater. 26 (17) (2014) 4970–4977, https://doi.org/10.1021/cm5018135.
[168] U. Zachwieja, H. Jacobs, CuTaN2, a copper (I)-tantalum (V)-nitride with delafossite structure, Eur. J. Solid State Inorg. Chem. 28 (1991) 1055–1062. http://inis.iaea.org/Search/search.aspx?orig_q=RN:23018494 (accessed September 10, 2020).
[169] M. Yang, A. Zakutayev, J. Vidal, X. Zhang, D.S. Ginley, F.J. Disalvo, Strong optical absorption in $CuTaN_2$ nitride delafossite, Energy Environ. Sci. 6 (2013) 2994–2999, https://doi.org/10.1039/c3ee40621k.
[170] R. Niewa, F.J. DiSalvo, Breaking up chains: the nitridocuprates(I) Ba[CuN] Ba16[(CuN)8][Cu2N3][Cu3N4] and Ca4Ba[CuN2]2, J. Alloys Compd. 279 (1998) 153–160. https://doi.org/10.1016/S0925-8388(98)00657-4.
[171] W. Sachsze, R. Juza, Metallamide und Metallnitride, 21. Mitteilung. Über Mischkristalle der Zusammensetzung (Li, Co)3N, (Li, Ni)3N und (Li, Cu)3N, Zeitschrift Für Anorg. Chemie. 259 (1949) 278–290. https://doi.org/10.1002/zaac.19492590510.
[172] R. Juza, K. Langer, K. Von Benda, Ternary Nitrides, Phosphides, and Arsenides of Lithium, Angew. Chemie Int. Ed. English. 7 (5) (1968) 360–370, https://doi.org/10.1002/(ISSN)1521-377310.1002/anie.v7:510.1002/anie.196803601.
[173] F.J. DiSalvo, S.S. Trail, H. Yamane, N.E. Brese, The crystal structure of $Sr_6Cu_3N_5$ with isolated, bent $(Cu_2^1N_3)^{7-}$ anions and the single crystal structural determination of SrCuN, J. Alloys Compd. 255 (1-2) (1997) 122–129, https://doi.org/10.1016/S0925-8388(96)02811-3.
[174] H. Yamane, F.J. DiSalvo, Sodium flux synthesis of nitrides, Prog. Solid State Chem. 51 (2018) 27–40, https://doi.org/10.1016/j.progsolidstchem.2017.08.002.
[175] In reference 159 also CuCaN was mentioned which apparently forms linear chains. However, the source: J. Jäger, PhD Thesis, 'Nitride und Nitridoverbindungen in Systemen Li-(Ca, Sr, Ba)-(Cu, Ag, Au)-N' Technische Hochschule Darmstadt, 1995 was not accessabl, n.d.
[176] N.V.S. Harisomayajula, S. Makovetskyi, Y. Tsai, Cuprophilic Interactions in and between Molecular Entities, Chem. – A Eur. J. 25 (2019) 8936-8954 and references therein. https://doi.org/10.1002/chem.201900332.
[177] H. Yamane, S. Sasaki, S. Kubota, M. Shimada, T. Kajiwara, Synthesis and crystal structure analysis of $Sr_8Cu_3In_4N_5$ and $Sr_{0.53}Ba_{0.47}CuN$, J. Solid State Chem. 170 (2) (2003) 265–272, https://doi.org/10.1016/S0022-4596(02)00083-X.
[178] H. Yamane, S. Sasaki, S.-ichi. Kubota, R. Inoue, M. Shimada, T. Kajiwara, Synthesis and Structure of $Ba_8Cu_3In_4N_5$ with Nitridocuprate Groups and One-Dimensional Infinite Indium Clusters, J. Solid State Chem. 163 (2) (2002) 449–454, https://doi.org/10.1006/jssc.2001.9424.
[179] H. Yamane, S. Sasaki, S. Kubota, T. Kajiwara, M. Shimada, $Ba_{14}Cu_2In_4N_7$, a new subnitride with isolated nitridocuprate groups and indium clusters, Acta Crystallogr. C. 58 (4) (2002) i50–i52, https://doi.org/10.1107/S010827010200361X.
[180] R.J. Wilson, B. Weinert, S. Dehnen, Recent developments in Zintl cluster chemistry, Dalt. Trans. 47 (42) (2018) 14861–14869, https://doi.org/10.1039/C8DT03174F.
[181] R. Niewa, Metal-Rich Ternary Perovskite Nitrides, Eur. J. Inorg. Chem. 2019 (32) (2019) 3647–3660, https://doi.org/10.1002/ejic.201900756.
[182] Y. Kim, B.J. Wieder, C.L. Kane, A.M. Rappe, Dirac Line Nodes in Inversion-Symmetric Crystals, Phys. Rev. Lett. 115 (2015), https://doi.org/10.1103/PhysRevLett.115.036806 036806.
[183] R. Yu, H. Weng, Z. Fang, X. Dai, X. Hu, Topological Node-Line Semimetal and Dirac Semimetal State in Antiperovskite Cu_3PdN, Phys. Rev. Lett. 115 (2015), https://doi.org/10.1103/PhysRevLett.115.036807 036807.
[184] C.X. Quintela, N. Campbell, D.F. Shao, J. Irwin, D.T. Harris, L. Xie, T.J. Anderson, N. Reiser, X.Q. Pan, E.Y. Tsymbal, M.S. Rzchowski, C.B. Eom, Epitaxial thin films of Dirac semimetal antiperovskite Cu_3PdN, APL Mater. 5 (9) (2017) 096103, https://doi.org/10.1063/1.4992006.
[185] N.J. Szymanski, L.N. Walters, O. Hellman, D. Gall, S.V. Khare, Dynamical stabilization in delafossite nitrides for solar energy conversion, J. Mater. Chem. A. 6 (42) (2018) 20852–20860, https://doi.org/10.1039/C8TA07536K.
[186] I. Ohkubo, T. Mori, Anisotropic Anomalies of Thermoelectric Transport Properties and Electronic Structures in Layered Complex Nitrides AMN_2 (A = Na, Cu; M = Ta, Nb), Chem. Mater. 27 (21) (2015) 7265–7275, https://doi.org/10.1021/acs.chemmater.5b02015.
[187] B. Sanchez-Lengeling, A. Aspuru-Guzik, Inverse molecular design using machine learning: Generative models for matter engineering, Science. 361 (6400) (2018) 360–365, https://doi.org/10.1126/science:aat2663.
[188] J. Noh, J. Kim, H.S. Stein, B. Sanchez-Lengeling, J.M. Gregoire, A. Aspuru-Guzik, Y. Jung, A. Com, Inverse Design of Solid-State Materials via a Continuous Representation, Matter. 1 (2019) 1370–1384, https://doi.org/10.1016/j.matt.2019.08.017.
[189] W. Sun, C.J. Bartel, E. Arca, S.R. Bauers, B. Matthews, B. Orvañanos, B.-R. Chen, M.F. Toney, L.T. Schelhas, W. Tumas, J. Tate, A. Zakutayev, S. Lany, A.M. Holder, G. Ceder, A map of the inorganic ternary metal nitrides, Nat. Mater. 18 (7) (2019) 732–739, https://doi.org/10.1038/s41563-019-0396-2.
[190] W. Shockley, H.J. Queisser, Detailed balance limit of efficiency of *p-n* junction solar cells, J. Appl. Phys. 32 (3) (1961) 510–519, https://doi.org/10.1063/1.1736034.